minerals

MDPI

Review

Precambrian Tectonic Affinity of Hainan and Its Evolution from Columbia to Rodinia

Limin Zhang [1,2], Xiang Cui [2,*], Yong Yang [1], Si Chen [1,*], Bin Zhao [1] and Xiguang Deng [1]

[1] Key Laboratory of Marine Mineral Resources, Ministry of Natural Resources, Guangzhou Marine Geological Survey, Guangzhou 511458, China; zhanglm8@mail2.sysu.edu.cn (L.Z.); yong0913029@163.com (Y.Y.); zbin_a@mail.cgs.gov.cn (B.Z.); dengxg68@163.com (X.D.)

[2] Guangdong Provincial Key Lab of Geodynamics and Geohazards, School of Earth Sciences and Engineering, Sun Yat-sen University, Guangzhou 510275, China

* Correspondence: cuixiang@tongji.edu.cn (X.C.); chen_si@vip.163.com (S.C.)

Abstract: The assembly and break-up of supercontinents have been hot research topics in international earth sciences because they represent a breakthrough in reconstructing the history of continental evolution and deepening the theory of plate tectonics, which is of indispensable importance to the development of earth sciences. With the continuous enrichment of paleomagnetic, paleontological, chronological, and geochemical data in the last two decades, the evolution of the supercontinent from Columbia to Rodinia has gradually gained unified understanding, and the reconstruction of the major plates within the supercontinent has basically been constrained. In contrast, the reconstruction of microplates, such as South China, Tarim, and Kabul, is controversial and has now become a popular topic and frontier area of supercontinent reconstruction. Hainan lies at the southern tip of South China, and a few Proterozoic units are exposed on the island. At present, Hainan is often taken as a part of the Cathaysia Block. However, due to the lack of exposed Mesoproterozoic igneous and supercrustal rocks in Cathaysia, the reconstruction model of the Cathaysia Block and even the South China Craton based solely on Mesoproterozoic units in Hainan are distinct from those based on units in the Yangtze Block and younger Proterozoic units within the Cathaysia Block, which makes the paleoposition of the South China Craton controversial. In this paper, we provide new detrital zircon U–Pb age data for the Baoban Complex, Hainan, together with the available data to comment on the affinities between Hainan and the Yangtze and Cathaysia Blocks in the Proterozoic, and on this basis, we can reconstruct the South China Craton within the Proterozoic supercontinents.

Keywords: detrital zircon; supercontinent cycle; Hainan; Proterozoic

check for updates

Citation: Zhang, L.; Cui, X.; Yang, Y.; Chen, S.; Zhao, B.; Deng, X. Precambrian Tectonic Affinity of Hainan and Its Evolution from Columbia to Rodinia. *Minerals* **2023**, *13*, 1237. https://doi.org/10.3390/min13101237

Academic Editor: Simon Paul Johnson

Received: 14 August 2023
Revised: 7 September 2023
Accepted: 20 September 2023
Published: 22 September 2023

Copyright: © 2023 by the authors. Licensee MDPI, Basel, Switzerland. This article is an open access article distributed under the terms and conditions of the Creative Commons Attribution (CC BY) license (https://creativecommons.org/licenses/by/4.0/).

1. Introduction

The South China Block (SCB) is an important part of the East Asian continent, formed by the collision of the Yangtze and Cathaysia Blocks along the Jiangnan (or Sibao) orogenic belt in the early Neoproterozoic (Figure 1a) [1–5]. A rich Precambrian geological record is preserved within the SCB, which is thought to have been involved in the evolution of the supercontinents from Columbia to Rodinia [6–28]. However, whether the SCB lies within or on the margin of the supercontinents is still highly controversial (see [8,29–36]). Hainan lies at the southern tip of the South China continent and plays an important role in reconstructing the SCB in Proterozoic supercontinents (Figure 1b,c) [6,8,37–41]. Sporadic Mesoproterozoic geochronological data led to early suggestions of a Grenvillian-age Sibao orogenic belt in South China [8]. And based on the comparable geochronological and geochemical records between the Mesoproterozoic Baoban Complex in Hainan and the Purcell Belt Supergroup in West Laurentia, as well as the Sibao orogenic belt, the SCB was placed in an internal location adjacent to Laurentia in the early Neoproterozoic (Figure 2a) [6,8,37]. However, an increasing number of studies conclude that the assembly between the Yangtze and Cathaysia blocks did not end until approximately 825–805 Ma [10,42–48], and the

Grenvillian orogenic belt did not exist in South China [47], supporting that the SCB is located at the margin of the Rodinia supercontinent (Figure 2b) [12,31,33,46–48]. Recently, some studies have gradually recognized the differences between the Yangtze and Cathaysia blocks during the Proterozoic, separated and reorganized the metasedimentary rock units within the SCB, and reanalyzed the possible position of the SCB within the supercontinent on the basis of a comprehensive understanding of the tectonic properties of each unit [27,40]. This paper presents a new study on sample 14HN-08A from the Mesoproterozoic Baoban Complex in west Hainan, South China. Based on the new U–Pb age data, as well as the published data from both Hainan and potential neighboring continents, we present an updated interpretation of Hainan Proterozoic tectonics and their possible paleogeographic connections with other continents during Precambrian supercontinent cycles.

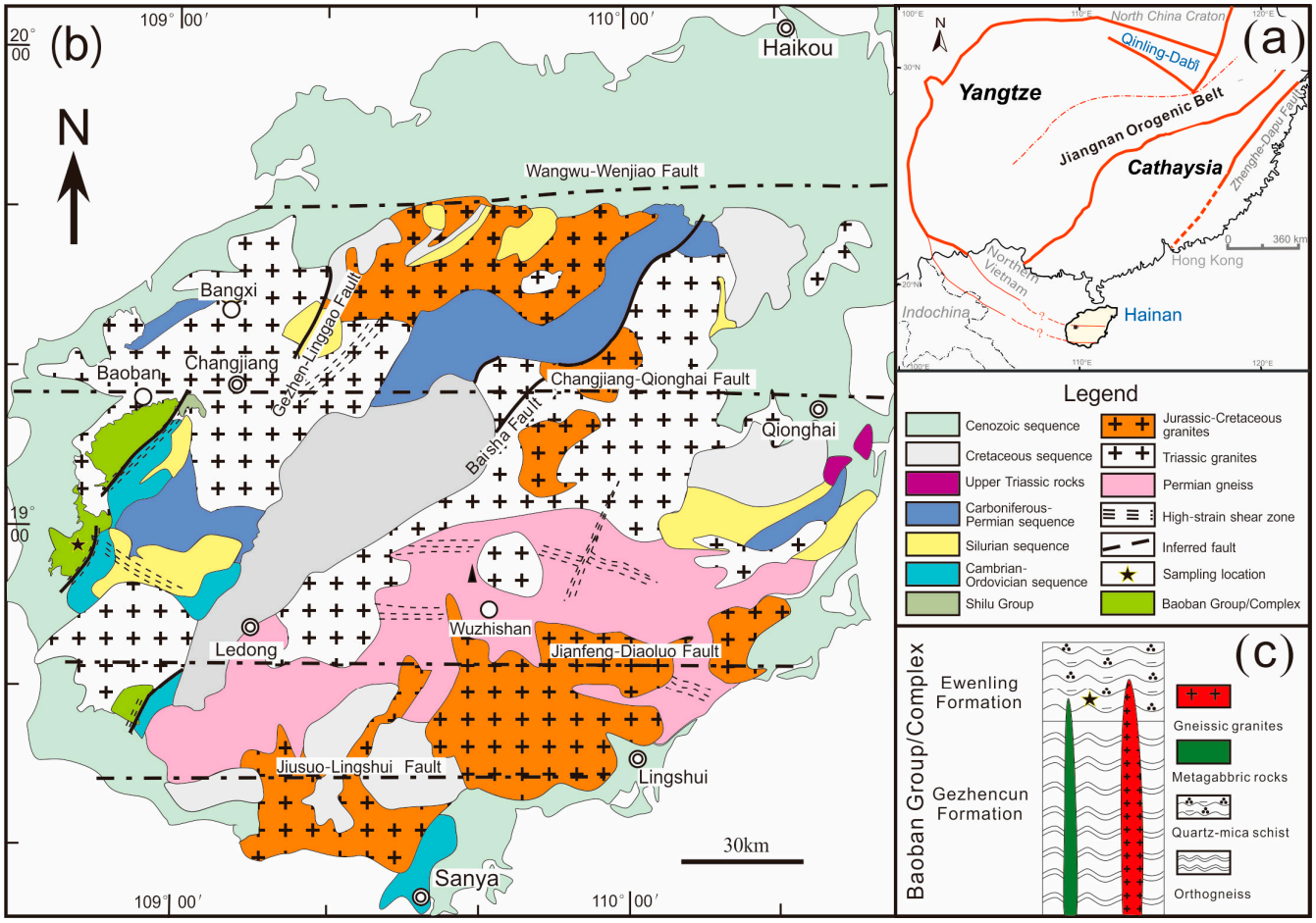


Figure 1. (**a**) Tectonic outline of the South China Craton (after [49]), (**b**) simplified geological map of Hainan Island showing the distribution of Mesoproterozoic rocks (revised after [50]), and (**c**) simplified stratigraphic column of the Mesoproterozoic Baoban Complex (revised after [50]).

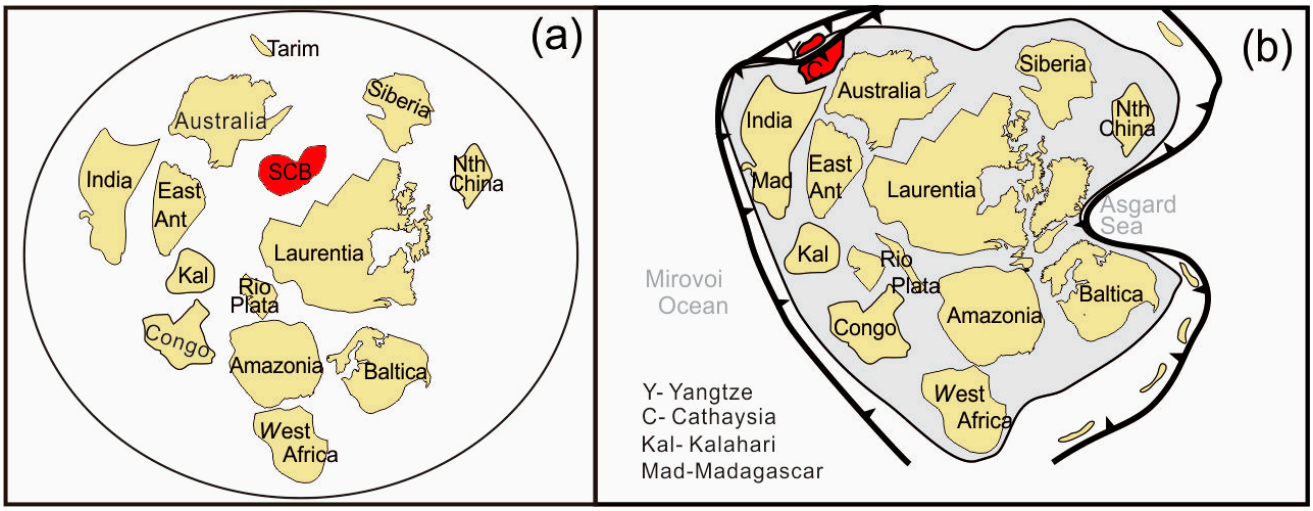


Figure 2. Representative models showing the location of the South China block in Rodinia (after [8,31]). Panel (**a**) shows internal locations and panel (**b**) shows external locations of the South China block in Rodinia.

2. Geological Setting and Sampling

Hainan constitutes the southern exposed extent of the SCB and is geographically connected to the South China mainland by the Qiongzhou Strait (Figure 1b). Some researchers have argued that Hainan was already part of the Cathaysia Block during the Proterozoic (e.g., [6,8,51]) and reconstructed the connection between Cathaysia and Laurentia in Columbia on the basis of the Mesoproterozoic metamafic rocks in Hainan [8,37–39]. However, another group of researchers believes that Hainan consists of two different blocks in the north and south [52,53], with the northern part of Hainan belonging to the SCB and the southern part of Hainan belonging to the Indochina Block [54] or Western Australia [53]. The two blocks were not fully integrated until the Mesozoic [55] or the early Paleozoic [53] along the Jiusuo–Lingshui fracture zone. Others divided Hainan Island into northwestern and southeastern terranes, which sutured along the northeast-southwest-trending Baisha Fault during the late Paleozoic [56,57]).

Precambrian units in Hainan are only sporadically exposed in the southwestern part of Hainan and are tectonically located to the south of the Changjiang–Qionghai fracture zone and to the north of the Jiusuo–Lingshui fracture zone (Figure 1b). They consist of three major units, including the Baoban Complex, Shilu Group, and Shihuiding Formation [58,59]. Both the Shilu Group and the overlying Shihuiding Formation only occur in the Shilu Fe-Co-Cu ore district of western Hainan. They are dominated by siliciclastic and carbonate rocks and have been interpreted as Mesoproterozoic or early Neoproterozoic units [8,37,59–61]. The Baoban Complex is exposed sporadically in southwest Hainan and is the oldest unit recognized [58,62]. It consists mainly of supracrustal rocks, granitoids, and metamafic rocks and has experienced strong deformation and metamorphosed to upper amphibolite facies, resulting in migmatized gneisses and various schists. The tectonostratigraphic relationships between these units and the chronostratigraphic framework of metasedimentary rocks have long been controversial because of poor outcropping and chronological constraints. Initially, Xia et al. [63] considered the "Baoban Group" as a schist system modified by migmatization, while Shan [64] pointed out that the "Baoban Group" consisted of two parts, including the lower part of plagiogneiss and the upper part of schist. Ye et al. [65] considered it to be a migmatite, while Yu et al. [66] believed that it was mainly a granitic intrusion in the Mesoproterozoic. Hou et al. [67] and Liang [68] considered that the "Baoban Group" is dominated by granitic rocks, while the residual amphibolite was considered as barbertonite, and the whole "Baoban Group" was treated as a granite–greenstone belt. This has led to the realization that the "Baoban Group" is a set of granite–greenstone assemblages [66–69]. The Guangdong District Survey Team in Hainan described the "Baoban Group" as a Cambrian

unit. The zircon U–Pb age of migmatite reported by Ye et al. [64] constrained the "Baoban Group" to the Meso-Neoproterozoic. Hou et al. [67] classified the amphibolite into the Paleoproterozoic and the granitic gneisses into the Mesoproterozoic with Sm–Nd ages of 1699 ± 3 Ma and 1379 ± 25 Ma, respectively. It can be seen that the disagreement mainly focuses on the age of each component unit of the "Baoban Group" and the relationship between them. With the continuous improvement of analytical methods and in-depth research, an increasing number of researchers have gradually realized that the "Baoban Group" mainly consists of supracrustal rocks and later intruded granitic and metamafic rocks and named it the "Baoban Complex" [37–39,52,60,70,71]. The supracrustal rocks are divided from bottom to top into the Gezhencun and Ewenling formations, and they were intruded by gneissic granitoids and amphibolites.

The metasedimentary sample analyzed in this study was collected from the Baoban Complex as shown in Figure 1. It is dominated by mica-quartz schists, composed of recrystallized quartz and plagioclase with biotite aligned along the schistosity plane.

3. Analytical Methods

Zircon grains from the sample were separated using heavy liquid and magnetic techniques and then handpicked under a binocular microscope. Their internal texture was examined by cathodoluminescence (CL) imaging using a scanning electron microprobe at the School of Earth Science and Engineering at Sun Yat-sen University. The operating conditions were an accelerating voltage of 15 Kv and a sample current of 10 nA with a beam diameter ranging from 1 to 5 μm. Zircon U-Pb dating was conducted by a laser ablation inductively coupled plasma mass spectrometry (LA-ICPMS) at the State Key Laboratory of Geological Processes and Mineral Resources, China University of Geosciences in Wuhan, China. The instrumental settings and detailed analytical procedures are outlined in [72,73]. A laser repetition rate of 8 Hz with a spot size of 32 μm was used for ablating the zircons. Fractionation correction and subsequent calculations follow ICPMSDataCal (8.4) [73]. Data reduction was carried out using the Ludwig SQUID 1.0 and ISOPLOT program [74]. All measurements were monitored using standard zircons GJ-1 (608.53 ± 0.37 Ma [75]) and 91,500 (1062.4 ± 0.6 Ma [76]). Individual analyses in the data table are presented with 1 σ error. Apparent ages are based on the $^{207}Pb/^{206}Pb$ ages and relative probability versus age diagrams are based on spots with discordance <10%.

4. Tectonostratigraphic Relationships between the Baoban Complex, the Shilu Group, and the Shihuiding Formation

Ages from 69 grains from sample 14HN-08A yield 64 concordant results (Table 1). They are concentrated in the range of 2700–1430 Ma, forming a major age peak at ~1800 Ma and subordinate peaks at ~1610 Ma and ~1460 Ma, consistent with those in Yao et al. [37] and Zhang et al. [39]. The four youngest grains define the youngest age cluster and yield a weighted mean age of 1451 ± 45 Ma (MSWD = 1.6). Together with the U–Pb age data of authigenic monazite reported by [41], the Ewenling Formation that was metamorphosed to lower amphibolite facies should have been deposited during 1450–1300 Ma. The lower Gezhencun Formation in the Baoban Complex, which was metamorphosed to upper amphibolite facies, was deposited at 1550–1450 Ma [41]. Metamafic and granitic rocks are preserved as lenses, pods, and interlayers with exposure scales ranging from a few meters to hundreds of meters [38,39] and were emplaced at 1441–1424 Ma [38,41] and 1450–1421 Ma [6,39,41], respectively. Gneissic granites emplaced at 1550 Ma published by [41] is the oldest unit in the Baoban Complex.

Table 1. Zircon U–Pb dating results for the representative sample from the metasedimentary rocks in Baoban Complex, west Hainan.

Spots	Th/U	Isotopic Ratios						Apparent Age (Ma)						Conc. (%)
		$^{207}Pb/^{206}Pb$	1σ	$^{207}Pb/^{235}U$	1σ	$^{206}Pb/^{238}U$	1σ	$^{207}Pb/^{206}Pb$	1σ	$^{207}Pb/^{235}U$	1σ	$^{206}Pb/^{238}U$	1σ	
14HN08A-01	0.13	0.110391	0.003417	4.888821	0.186053	0.316883	0.008564	1806	28	1800	16	1774	21	98
14HN08A-02	0.60	0.091579	0.002202	3.064874	0.078118	0.239100	0.003460	1459	23	1424	10	1382	9	97
14HN08A-03	0.21	0.104282	0.002610	4.442245	0.122251	0.304680	0.004636	1702	23	1720	12	1714	12	99
14HN08A-04	0.18	0.092747	0.002259	3.271280	0.081521	0.252133	0.003487	1483	23	1474	10	1449	9	98
14HN08A-05	0.28	0.148786	0.003995	8.802123	0.265802	0.422676	0.008113	2332	23	2318	14	2273	19	98
14HN08A-06	0.20	0.105382	0.002955	4.247538	0.126591	0.288213	0.004859	1721	26	1683	12	1633	12	96
14HN08A-07	0.45	0.126045	0.003178	6.450614	0.208443	0.364465	0.007476	2044	22	2039	14	2003	18	98
14HN08A-08	0.12	0.099923	0.002337	3.899537	0.092149	0.279211	0.003796	1633	19	1614	10	1587	10	98
14HN08A-09	0.13	0.098673	0.002679	2.868054	0.082726	0.207514	0.003271	1599	26	1374	11	1216	9	87
14HN08A-10	0.33	0.110066	0.002968	4.566179	0.120221	0.298004	0.004774	1811	25	1743	11	1681	12	96
14HN08A-11	0.49	0.166655	0.003879	9.461348	0.237984	0.406913	0.007591	2524	20	2384	12	2201	18	92
14HN08A-12	0.18	0.108933	0.002681	4.637195	0.124589	0.305042	0.005320	1783	23	1756	11	1716	13	97
14HN08A-13	0.12	0.110998	0.002852	4.870599	0.135393	0.314555	0.005656	1817	24	1797	12	1763	14	98
14HN08A-14	0.26	0.112970	0.003315	4.893483	0.149539	0.310367	0.005311	1848	27	1801	13	1743	13	96
14HN08A-15	0.35	0.107964	0.003262	4.561516	0.141800	0.303948	0.005987	1765	28	1742	13	1711	15	98
14HN08A-16	0.27	0.173166	0.004628	11.209902	0.299045	0.465195	0.008037	2589	23	2541	13	2462	18	96
14HN08A-17	0.13	0.089327	0.002206	2.934309	0.076850	0.235910	0.003791	1413	23	1391	10	1365	10	98
14HN08A-18	0.17	0.112775	0.003111	5.004778	0.136219	0.320324	0.005907	1856	25	1820	12	1791	15	98
14HN08A-19	0.65	0.107003	0.002866	4.559442	0.135397	0.305526	0.005769	1750	25	1742	13	1719	14	98
14HN08A-20	0.39	0.106852	0.002959	4.003608	0.108747	0.269608	0.003949	1747	26	1635	11	1539	10	93
14HN08A-21	1.10	0.100558	0.003423	3.995998	0.148806	0.286657	0.005684	1635	32	1633	15	1625	14	99
14HN08A-22	0.29	0.101781	0.002537	4.081697	0.106479	0.288315	0.004457	1657	23	1651	11	1633	11	98
14HN08A-23	0.46	0.112227	0.003025	4.848394	0.150569	0.309636	0.005495	1836	24	1793	13	1739	14	96
14HN08A-24	0.62	0.100131	0.002855	3.950613	0.106366	0.286253	0.005692	1628	27	1624	11	1623	15	99
14HN08A-25	0.35	0.106548	0.003003	4.497571	0.130471	0.305009	0.005366	1743	26	1731	12	1716	14	99
14HN08A-26	0.36	0.113004	0.002613	5.053766	0.124571	0.322390	0.005333	1850	24	1828	11	1801	13	98
14HN08A-27	0.23	0.131412	0.003188	6.851896	0.215336	0.373391	0.007570	2117	22	2092	14	2045	18	97
14HN08A-28	0.73	0.131544	0.003451	6.776983	0.209066	0.370571	0.006873	2120	23	2083	14	2032	16	97
14HN08A-29	0.12	0.125223	0.003926	5.065787	0.163586	0.290387	0.004981	2032	28	1830	14	1643	13	89
14HN08A-30	0.63	0.119689	0.002980	5.569381	0.137450	0.334355	0.004528	1952	22	1911	11	1859	11	97
14HN08A-31	0.43	0.110923	0.002637	4.573429	0.105940	0.296187	0.004072	1815	22	1744	10	1672	10	95
14HN08A-32	0.21	0.136012	0.003810	5.514224	0.183067	0.290779	0.006322	2177	25	1903	15	1645	16	85
14HN08A-33	0.29	0.112868	0.003773	4.690151	0.129880	0.299203	0.006614	1846	30	1765	12	1687	17	95
14HN08A-34	0.03	0.099340	0.002705	3.364121	0.088623	0.243083	0.003422	1613	25	1496	11	1403	9	93
14HN08A-35	0.17	0.110126	0.002834	4.484906	0.112308	0.292395	0.004251	1811	24	1728	11	1653	11	95
14HN08A-36	0.55	0.106390	0.002635	4.521962	0.111496	0.305329	0.004385	1739	23	1735	11	1718	11	98
14HN08A-37	0.45	0.107477	0.005215	3.843943	0.171592	0.258438	0.006129	1767	45	1602	18	1482	16	92

Table 1. *Cont.*

Spots	Th/U	Isotopic Ratios						Apparent Age (Ma)						Conc. (%)
		$^{207}Pb/^{206}Pb$	1σ	$^{207}Pb/^{235}U$	1σ	$^{206}Pb/^{238}U$	1σ	$^{207}Pb/^{206}Pb$	1σ	$^{207}Pb/^{235}U$	1σ	$^{206}Pb/^{238}U$	1σ	
14HN08A-38	0.19	0.107828	0.002885	4.582684	0.159219	0.305804	0.008336	1765	25	1746	15	1720	21	98
14HN08A-39	0.31	0.183243	0.004152	12.982508	0.299290	0.509513	0.007207	2682	16	2678	11	2655	16	99
14HN08A-40	0.27	0.108819	0.002699	4.777753	0.122425	0.315847	0.005072	1780	21	1781	11	1769	13	99
14HN08A-41	0.11	0.114172	0.002934	5.210490	0.140242	0.329053	0.005448	1933	26	1854	12	1834	13	98
14HN08A-42	0.17	0.155685	0.004101	8.727132	0.245992	0.402439	0.006795	2410	22	2310	13	2180	16	94
14HN08A-43	0.51	0.110577	0.003643	4.538345	0.159670	0.294868	0.005607	1809	47	1738	15	1666	14	95
14HN08A-44	0.58	0.156180	0.003856	9.294805	0.237775	0.427330	0.006664	2415	22	2368	12	2294	15	96
14HN08A-45	0.40	0.104995	0.002961	3.730374	0.104457	0.255377	0.004195	1715	26	1578	11	1466	11	92
14HN08A-46	0.08	0.103778	0.002531	4.083607	0.099698	0.282370	0.003960	1694	23	1651	10	1603	10	97
14HN08A-47	0.47	0.110789	0.003502	4.966813	0.173641	0.320902	0.006119	1813	29	1814	15	1794	15	98
14HN08A-48	0.27	0.106560	0.002957	4.422248	0.119308	0.297691	0.004234	1743	23	1717	11	1680	11	97
14HN08A-49	0.41	0.113163	0.002972	5.041648	0.129648	0.319438	0.004455	1851	24	1826	11	1787	11	97
14HN08A-50	0.17	0.109477	0.003147	4.637338	0.134825	0.303623	0.004570	1790	26	1756	12	1709	12	97
14HN08A-51	0.50	0.113354	0.003396	5.099284	0.159473	0.323458	0.006079	1854	27	1836	14	1807	15	98
14HN08A-52	0.64	0.112721	0.003963	4.980168	0.166349	0.318353	0.005520	1844	29	1816	14	1782	14	98
14HN08A-53	0.12	0.099337	0.005568	3.890536	0.219526	0.278324	0.004306	1613	55	1612	23	1583	11	98
14HN08A-54	0.29	0.098160	0.003715	2.231728	0.079910	0.164172	0.002972	1591	36	1191	13	980	8	80
14HN08A-55	0.06	0.082548	0.003387	2.047297	0.091364	0.178475	0.002845	1258	40	1131	15	1059	8	93
14HN08A-56	0.52	0.097660	0.003726	3.793526	0.170664	0.278265	0.004975	1580	36	1591	18	1583	13	99
14HN08A-57	0.06	0.096737	0.002572	2.697794	0.076371	0.201170	0.002555	1562	23	1328	11	1182	7	88
14HN08A-58	0.23	0.097502	0.002552	3.153452	0.086808	0.233258	0.002930	1577	25	1446	11	1352	8	93
14HN08A-59	0.44	0.182704	0.005057	12.891229	0.371990	0.509445	0.007258	2677	23	2672	14	2654	16	99
14HN08A-60	0.26	0.108618	0.003001	4.725210	0.140880	0.313722	0.004891	1776	26	1772	13	1759	12	99
14HN08A-61	0.46	0.150141	0.004260	9.001626	0.263426	0.432850	0.006199	2347	24	2338	14	2319	14	99
14HN08A-62	0.16	0.118484	0.002726	5.065077	0.121935	0.308195	0.003661	1944	21	1830	10	1732	9	94
14HN08A-63	0.10	0.148682	0.003490	7.223811	0.172720	0.350679	0.005234	2331	18	2139	11	1938	13	90
14HN08A-64	0.43	0.104232	0.003002	3.868091	0.127274	0.267781	0.005228	1702	27	1607	14	1530	14	95
14HN08A-65	0.45	0.091060	0.001917	2.652901	0.060476	0.210483	0.002736	1448	20	1315	9	1231	8	93
14HN08A-66	0.19	0.099074	0.002159	3.868075	0.115254	0.279004	0.005294	1606	20	1607	12	1586	14	98
14HN08A-67	0.48	0.098061	0.002095	3.739914	0.118831	0.274032	0.005730	1587	20	1580	13	1561	15	98
14HN08A-68	0.12	0.141732	0.003810	7.229319	0.217186	0.368827	0.005864	2250	23	2140	14	2024	14	94
14HN08A-69	0.13	0.099061	0.002180	3.729650	0.089068	0.272095	0.003338	1606	21	1578	10	1551	9	98

The magmatic rocks within the Baoban Complex are dominated by contemporaneous metamafic rocks and A-type granite [8,38,39], forming a typical bimodal magmatic assemblage, supporting an extensional setting during the Mesoproterozoic. Previous regional investigations on Hainan have suggested that the Baoban Complex is in fault contact with the Shilu Group [58,59]. Due to the controversial depositional age of the Shilu Group, the tectonostratigraphic relationship between the Shilu Group, the Baoban Complex, and the Shihuiding Formation has not been well constrained. Li et al. [8] and Yao et al. [37] reported the Sensitive High Resolution Ion MicroProbe (SHRIMP) zircon U–Pb age of tuffs in the fifth layer of the Shilu Group to be 1439 ± 9 Ma, which is in line with the age of the Baoban Complex, and suggested that the lower five layers of the Shilu Group should have been deposited prior to ca. 1430 Ma. Furthermore, they limited the maximum depositional age of the sixth layer to 1063 ± 27 Ma based on the detrital zircon U-Pb age and thus considered that there was a sedimentary hiatus of no less than 400 Myr between the "fifth" and "sixth" layers of the Shilu Group, proposing that the sixth layer should be removed from the group and treated as a distinctive stratigraphic unit, namely the "Liuceng Formation". Wang et al. [60] suggested that the Shilu Group (layers 4–6) and the Shihuiding Formation were deposited ca. 1.0 Ga and proposed that the Shihuiding Formation should be considered as the top, i.e., the seventh layer of the Shilu Group, based on their similar zircon U–Pb age distributions.

The Baoban Complex experienced amphibolite facies metamorphism, whereas the Shilu Group displays modification to low-temperature green schist facies, with the two in fault contact [58,59]. This suggests that a tectonic-metamorphic event should have occurred in Hainan prior to the precipitation of the Shilu Group and after the formation of the Baoban Complex. Metamorphic zircons of 1300–1000 Ma are widely exposed in the metasedimentary rocks, gneisses, and magmatic rocks of the Baoban Complex but are largely absent within the Shilu Group (layers 3–6) [37–39,70,77] (Figure 2), which indicates that these sedimentary and magmatic rocks experienced metamorphism during 1300–1000 Ma. Abundant detrital zircon U–Pb data for layers 3–6 of the Shilu Group constrain the maximum depositional age of the mid-upper Shilu Group to approximately 1100 Ma [60,70,71]. All of these results support that the mid-upper Shilu Group is a depositional system distinctively different from the metasedimentary rocks in the Baoban Complex. No age data are currently available for the first and second layers of the Shilu Group because of poor outcrops.

Sedimentary detritus from layers 3–6 of the Shilu Group are of low maturity, relatively enriched in high field strength elements and rare earth elements, and deficient in transition elements (e.g., Sc and Co) [71], implying their origination dominantly from felsic igneous rocks. This inference further indicates their deposition on active continental margins [78–80]. The first to fifth layers of the Shilu Group are relatively strongly deformed and intensely metamorphosed, whereas the sixth layer of the Shilu Group shows weak deformation and slight metamorphism. The Shihuiding Formation is a suite of siliciclastic clastic rocks that are unmetamorphosed and less deformed [81]. In contrast to the Shilu Group, it has a higher quartz content, is enriched in SiO_2, and depleted in CaO, Na_2O, and TiO_2 with more remarkable differentiation between light and heavy rare earth elements [71,82], implying that it should originate dominantly from recycled sediments. Furthermore, it yields an additional age peak at ~1390 Ma and a slightly younger maximum depositional age of ~930 Ma [40,71] (Figure 3). Distinct metamorphic grades, sedimentary sources, and the unconformity between the Shilu Group and Shihuiding Formation argue against them as one unit.

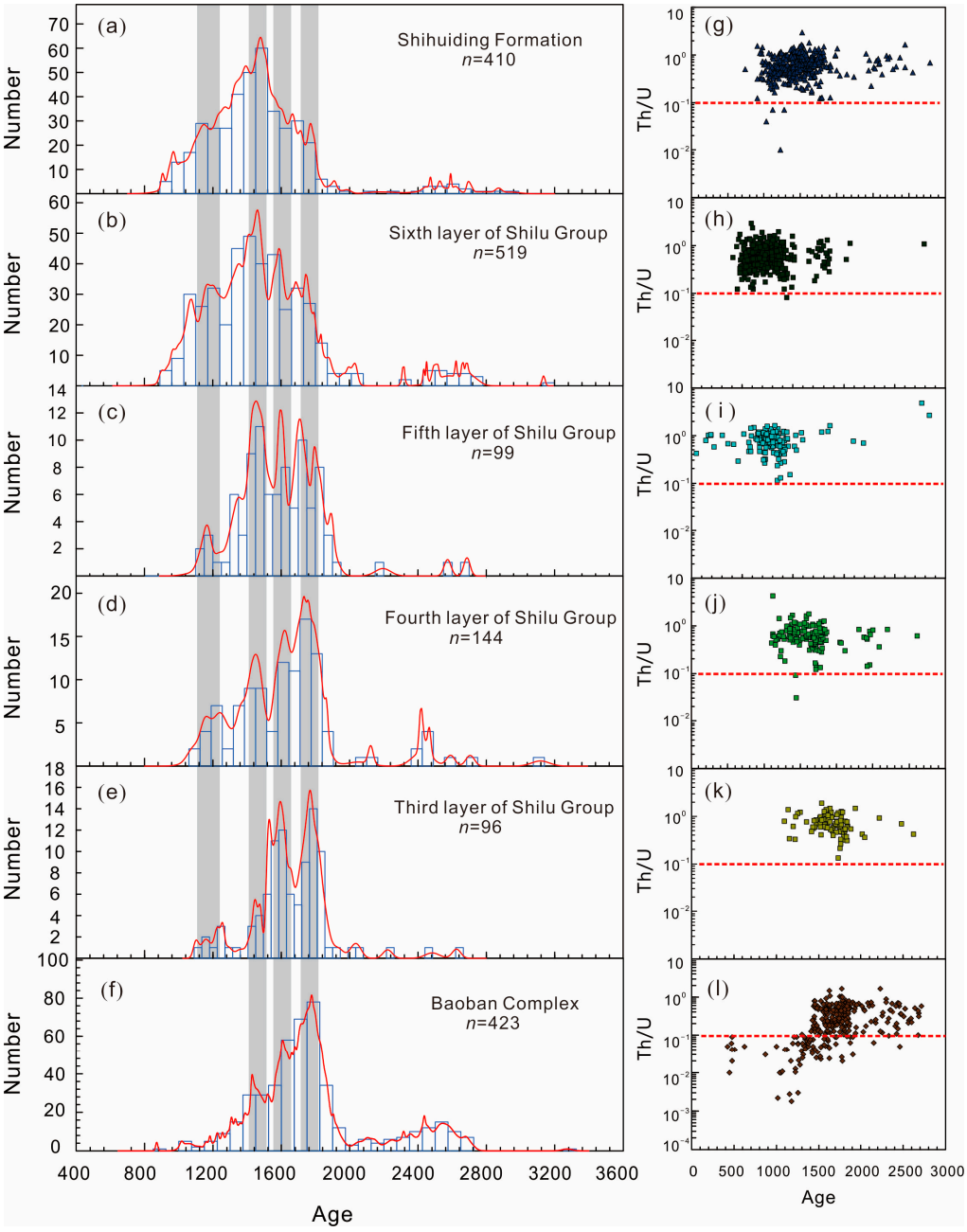


Figure 3. Relative probability density plots (**a**–**f**) and Th/U characteristics (**g**–**l**) for Proterozoic unit detrital zircons from Hainan (data from [37,39,41,60,71] and this study).

5. Correlation to Sequences in the Cathaysia and Yangtze Blocks

Hainan has long been considered a part of the Cathaysia Block, and the Baoban Complex has been used as critical evidence for delimiting the position of the Cathaysia Block and even the South China Block in Precambrian supercontinent reconstructions (e.g., [8,37]). However, there has been no relevant evidence to prove the affinity between Hainan and the Cathaysia Block during the Proterozoic. The Precambrian units within the Cathaysia Block are dominated by early Neoproterozoic igneous rocks and a series of middle to late Neoproterozoic sedimentary rocks (e.g., [10,11,45,46,83,84]), which are absent in Hainan; furthermore, neither Mesoproterozoic sedimentary nor igneous rocks that crop out in Hainan have been reported from the Cathaysia Block [2,4,25,37,38,83–90], casting doubt on the Mesoproterozoic-early Neoproterozoic Cathaysia-Hainan connection.

Available zircon U–Pb chronology and Hf isotope data show that detrital zircons in Hainan with age ranges of 1700–1100 Ma have dominantly positive $\varepsilon_{Hf}(t)$ values [61,71], and most of these zircons have crustal incubation times of less than 300 Ma, indicating an important period for juvenile crust generation. In contrast, the crust of the Cathaysia Block showed episodic accretion, with major crustal growth occurring ca. 2500 Ma and 1000 Ma [86–90]. Therefore, these differences in crustal evolution and diachronous magmatism and sequence imply that Hainan was not closely linked to the Cathaysia Block during the Proterozoic.

In contrast, the Kunyang and Huili Groups as well as the Julin Group developed at the southwest margin of the Yangtze Block were deposited at approximately 1050 Ma and are dominated by siliceous clastic rocks and carbonates, similar to the Shilu Group [91–95]. Detrital zircons from the two groups yield age peaks at 1750 Ma, 1600 Ma, 1450 Ma, and 1160 Ma [91–95] (Figure 4), which matches well with the Shilu Group. These similarities, together with the comparable Hf isotope compositions (Figure 4) and geochemical compositions [71], indicate that the Kunyang Group and its equivalent in the Yangtze Block share a similar provenance with the Shilu Group. Moreover, detrital zircons of 1700–1100 Ma with dominantly depleted Hf isotope compositions (Figure 5) suggest comparable juvenile crustal generation between Hainan and Yangtze during the Mesoproterozoic. The ca. 1430 Ma metamafic and granitic rocks in Hainan show geochemical compositions and Sr-Nd-Hf isotopic signatures comparable to those of the 1530–1375 Ma magmatic rocks in the southwest Yangtze Block [40,96,97]. In summary, Hainan shows obvious similarities with the Yangtze Block in terms of crustal evolution, magmatic assemblages, and sedimentary facies and provenance, implying that Hainan and Yangtze might constitute a single, spatially unified domain in the Proterozoic. This interpretation is also supported by the similar mineralization style of iron deposits hosted in the Shilu Group and ore deposits in the Dahongshan, Dongchuan, Hekou and Sin Quyen groups in the western Yangtze Block [98], although the age of the iron deposit in Hainan is poorly constrained.

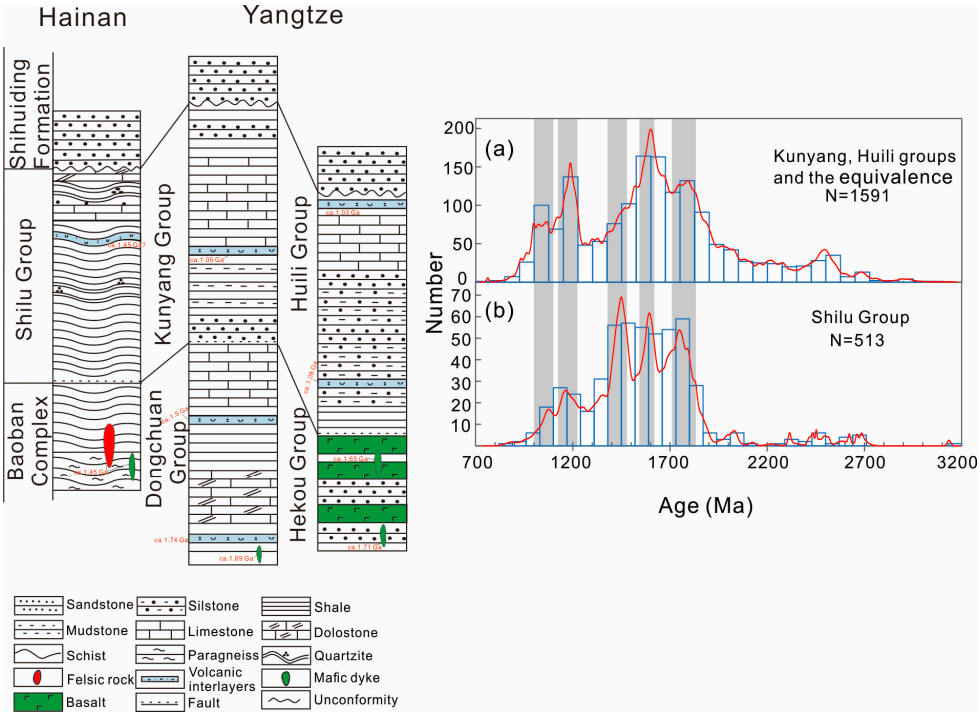


Figure 4. Simplified stratigraphic columns and relative probability density plots for the representative samples from the (**a**) Shilu Group in Hainan and (**b**) Kunyang and Huili groups in the Yangtze Block. Simplified stratigraphic column is modified after [13,69,71,93–95]. Data for the Shilu Group are from [37,60,71] and the Kunyang and Huili groups are from [23,91–95].

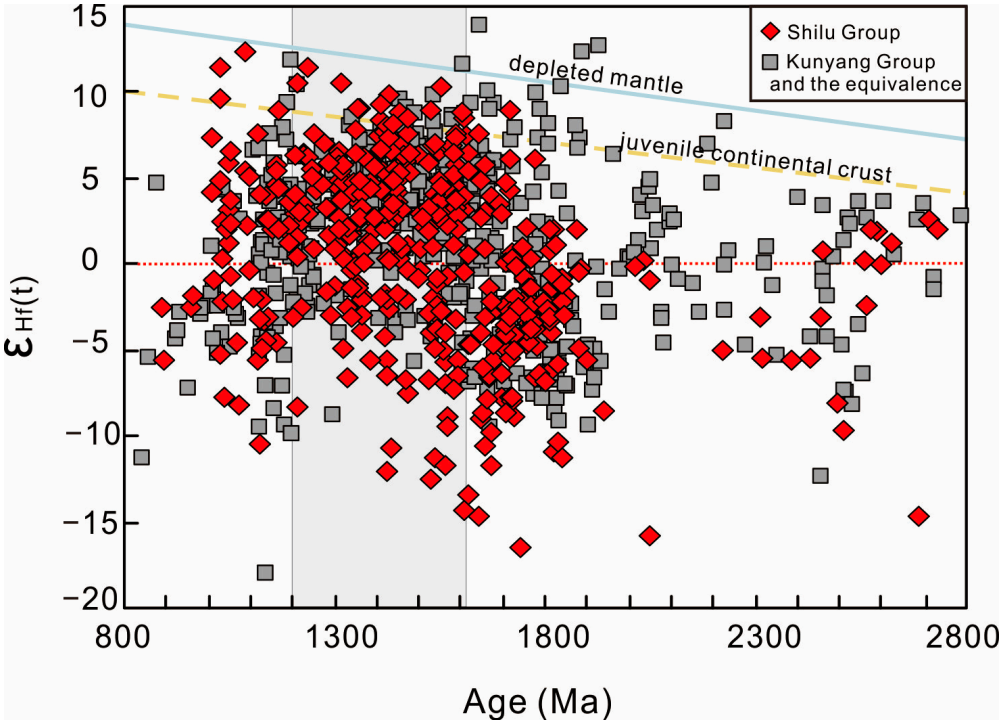


Figure 5. Hf isotopic composition of detrital zircon from the Shilu Group in Hainan and Kunyang and Huili groups in the Yangtze Block. Data for the Shilu Group are from [37,68,70] and the Kunyang and Huili groups are from [23,86,88].

6. Hainan and Precambrian Supercontinent Evolution

6.1. Reconstructing West Hainan–Yangtze in Columbia

A range of paleogeographic reconstructions have been proposed to reconstruct Columbia [34,99–101]. Combined with the available data on magmatism, sedimentary rocks, and paleomagnetism, it is usually believed that the Siberia–Laurentia–Baltica constitutes the core of Columbia [101], while the South American–West African, Western Australian–South African, East Antarctic, North China, and India blocks are located in the margins [34,99].

The Baoban metasedimentary rocks have comparable depositional ages to the Mesoproterozoic sedimentary sequences deposited across the western margin of Laurentia, e.g., the 1.47–1.40 Ga Belt-Purcell, the 1.46–1.42 Ga PR1, the 1.48–1.44 Ga Yankee Joe/Hess Canyon-Defiance, and the 1.47–1.45 Ga Trampas and Marquenas basins [102–109]. Detrital zircons from the Baoban Complex yield comparable age populations and Hf isotope compositions to those in the lower Belt–Purcell Supergroup and their equivalents [102–104,106–108,110] (Figure 5, date should be seen in Tables S1 and S2), which may have originated from the Gawler Craton [111–116] and East Antarctica [117–122], in which many Mesoproterozoic igneous rocks have been identified and reported. Additionally, the Mesoproterozoic metamafic and felsic rocks from the Baoban Complex in Hainan share similar geochronological and geochemical characteristics with those in the Belt–Purcell Supergroup [8,37–39,103,123–126]. Such similarities suggest the close spatial affinity of West Hainan with west Laurentia, the Gawler Craton, and East Antarctica, and thus Hainan was more likely located in the center of the Columbia supercontinent.

6.2. Reconstructing West Hainan–Yangtze in Rodinia

Detrital zircons from the Shilu Group mainly yield Paleoproterozoic to Mesoproterozoic ages with a few Archean dates, forming age peaks at ~1780 Ma, ~1600 Ma, ~1450 Ma, and ~1170 Ma [37,60,71] (Figure 6a). This is significantly different from the ~1100–1000 Ma Buffo Hump Formation (Deer Trail Group) and its equivalent units, which overlie the

Belt–Purcell Supergroup [104,105,127–129], but are comparable to the South Delhi Supergroup in NW India (Figure 7) [130–132] and its equivalent—the upper Vindhyan sequence of the Vindhyan Basin located in the central part of the Northern India [130–134]. All of these results suggest that the source of the Shilu Group is markedly different from that of the Buffo Hump Formation (Deer Trail Group) but similar to that of the South Delhi Supergroup and the upper Vindhyan sequence, perhaps due to Hainan having drifted away from the vicinity of western Laurentia and occupying an external position of the supercontinent, near the Indian Craton as shown in Figure 8, prior to ~1100 Ma.

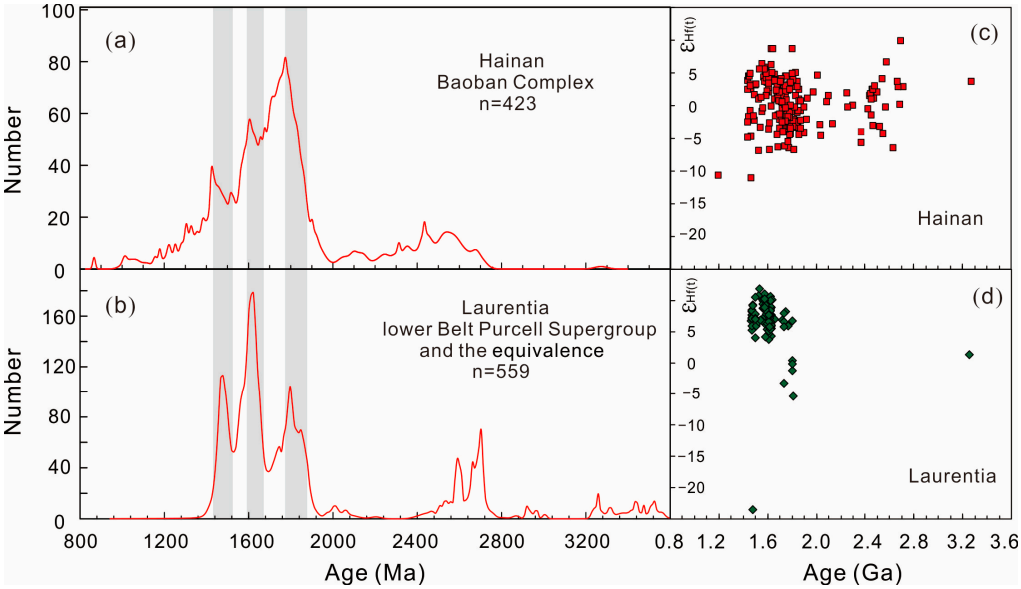


Figure 6. Comparisons of Mesoproterozoic sequences in west Hainan and Laurentia. (**a**,**b**) show age distribution and (**c**,**d**) show Hf isotopic composition of detrital zircon. Data for Hainan are from [37,39], West Laurent are from [103,106,108].

Globally, the 1200~1100 Ma magmatism occurred mainly in Laurentia, Baltica, Africa, South America, and East Antarctica [135–139]. Among these continents, Laurentia and East Antarctica are the most likely sources for detritus of Hainan–Yangtze–India. Because magmatic events at approximately 2100 Ma were widely developed in Africa and South America, the sources they provided tend to carry many zircon grains with ages of 2100 Ma, whereas detrital material from the Baltic Craton tends to contain large amounts of zircon grains of 1900 Ma [136,137,140,141] (Figure 8). Detrital zircons from the sedimentary sequence in Laurentia mainly yield age peaks at ~1700 Ma, ~1450 Ma, and 1250 Ma and essentially contain no zircons of 1650–1550 Ma [104,105,127–129], which is distinct from those of Hainan–Yangtze–India. Although much of Antarctica is covered with ice, abundant ~1200–1100 Ma igneous and metamorphic clasts have been identified in the Gamburtsev Subglacial Mountains [119,139,142]. Together with the ~1606–1595 Ma felsic volcanic rocks found in moraines of the Terre Adélie Craton [117], 1578 Ma granite clasts from the Transantarctic Mountains [118] and 1486–1404 Ma mafic and felsic rocks observed on Mount Brown [120–122], igneous zircons in East Antarctica, may have served as a vital source for Hainan–Yangtze–India during the late Mesoproterozoic.

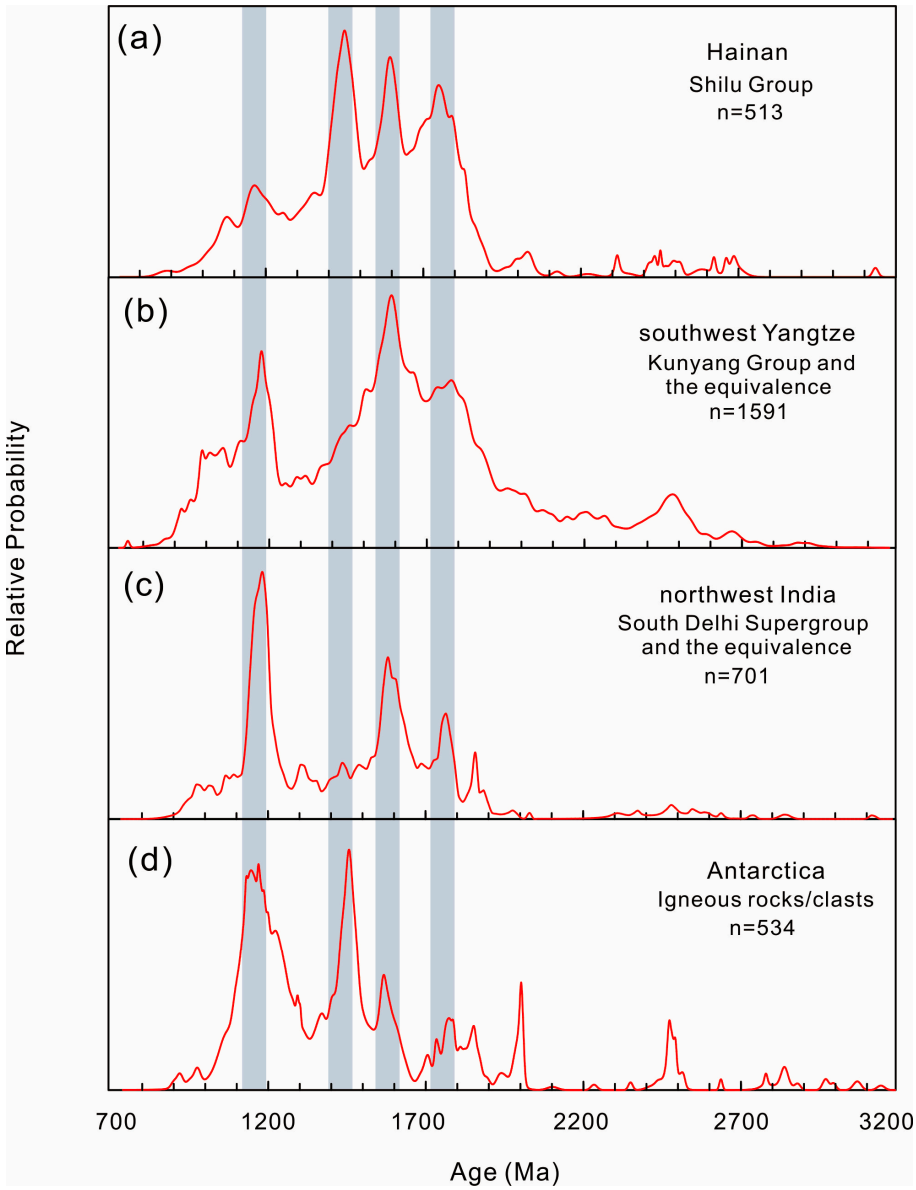


Figure 7. Relative probability plots for zircon ages for late Mesoproterozoic sequence in west Hainan (**a**), southwest Yangtze (**b**), northwest India (**c**), and Antarctica (**d**). Data in west Hainan are from [37,41] and this study; west Laurentia are from [104,106,108]; northwest India are from [129–132]; East Antarctica are from [117,119,137,141].

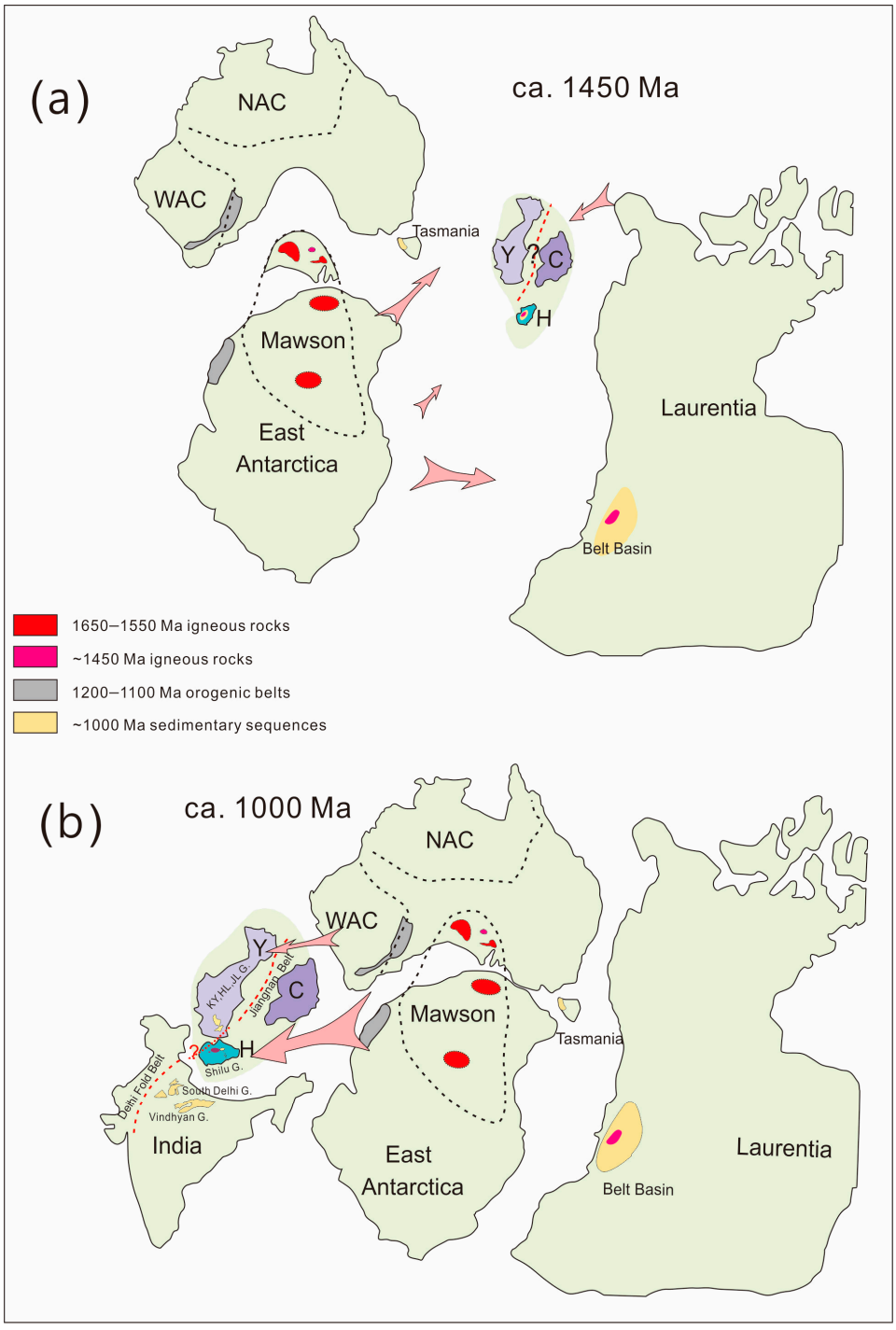


Figure 8. Proposed configuration of west Hainan, Yangtze, India, Mawson continent (South Australia Gawler Craton and Antarctica) and Laurentia during extension of supercontinent Columbia ca. 1450 Ma and (**a**) assembly of supercontinent Rodinia ~1000 Ma (**b**). Y-Yangtze Block, C-Cathaysia Block, H-Hainan, NAC-North Australian Craton, SAC-South Australia Craton, KY-Kunyang Group, HL-Huili Group, JL-Julin Group. Inferred extraneous sedimentary provenance links are shown by magenta arrows. Red ellipses circled with dashed line on Mawson continent depict point sources in East Antarctica and Terre Adélie of unknown extent (for interpretation of the references to color in this figure legend, the reader is referred to the web version of this article).

7. Conclusions

New U-Pb geochronology of zircon in metasedimentary rocks from the Mesoproterozoic Baoban Complex in SW Hainan, together with published data for South China, indicate the following:

1. There are three Proterozoic units in Hainan, including the Mesoproterozoic Baoban Complex, the late Mesoproterozoic Shilu Group, and the Neoproterozoic Shihuiding Formation.
2. Hainan was linked to the Yangtze Block rather than the Cathaysia Block in the late Mesoproterozoic–early Neoproterozoic.
3. The connected Hainan–Yangtze blocks likely drifted from the core to the margin of the supercontinents in the Proterozoic.

Supplementary Materials: The following are available online at https://www.mdpi.com/article/10.3390/min13101237/s1, Table S1: Published zircon U-Pb geochronological data of Meso-Neoproterozoic samples from the Hainan,Yangtze Block, India, western Laurentia and East Antarctica; Table S2: Published zircon Hf isotopic data of Meso-Neoproterozoic samples from the Hainan, Yangtze Block, India, western Laurentia and East Antarctica.

Author Contributions: Writing—original draft, data analysis, L.Z.; conceptualization, supervision, writing—reviewing and editing, L.Z. and X.C.; sample collection, sample preparation, L.Z.; conception of experiment, S.C.; data curation, Y.Y., B.Z. and X.D. All authors have read and agreed to the published version of the manuscript.

Funding: This study was jointly funded by the National Science Foundation of China (42102262, U2244222 and 42002237), the Scientific and Technological Planning Project of Guangzhou City (202201011487), and the China Geological Survey (DD20221718).

Data Availability Statement: The data presented in this work are available on request from the corresponding author.

Acknowledgments: We would like to thank G-F Zhao and H-Y He for their help during field work. We also appreciate the editor and two anonymous reviewers who have provided insightful suggestions, which greatly improved the manuscript.

Conflicts of Interest: The authors declare no conflict of interest.

References

1. Greentree, M.R.; Li, Z.X.; Li, X.H.; Wu, H. Late Mesoproterozoic to earliest Neoproterozoic basin record of the Sibao orogenesis in western South China and relationship to the assembly of Rodinia. *Precambrian Res.* **2006**, *151*, 79–100. [CrossRef]
2. Li, Z.X.; Li, X.H. Formation of the 1300-km-wide intracontinental orogen and postorogenic magmatic province in Mesozoic South China: A flat-slab subduction model. *Geology* **2007**, *35*, 179–182. [CrossRef]
3. Ye, M.F.; Li, X.H.; Li, W.X.; Liu, Y.; Li, Z.X. SHRIMP zircon U-Pb geochronological and whole-rock geochemical evidence for an early Neoproterozoic Sibaoan magmatic arc along the southeastern margin of the Yangtze Block. *Gondwana Res.* **2007**, *12*, 144–156. [CrossRef]
4. Shu, L.S.; Deng, P.; Yu, J.H.; Wang, Y.B.; Jiang, S.Y. The age and tectonic environment of the rhyolitic rocks on the western side of Wuyi Mountain, South China. *Sci. China (Ser. D)* **2008**, *51*, 1053–1063. [CrossRef]
5. Shu, L.S.; Wang, J.Q.; Yao, J.L. Tectonic evolution of the eastern Jiangnan region, South China: New findings and implications on the assembly of the Rodinia supercontinent. *Precambrian Res.* **2019**, *322*, 42–65. [CrossRef]
6. Li, Z.X.; Li, X.H.; Zhou, H.W.; Kinny, P.D. Grenvillian continental collision in south China: New SHRIMP U-Pb zircon results and implications for the configuration of Rodinia. *Geology* **2002**, *30*, 163–166. [CrossRef]
7. Li, X.H.; Qi, C.S.; Liu, Y.; Liang, X.R.; Tu, X.L.; Xie, L.W.; Yang, Y.H. Petrogenesis of the Neoproterozoic bimodal volcanic rocks along the western margin of the Yangtze Block: New constraints from Hf isotopes and Fe/Mn ratios. *Chin. Sci. Bull.* **2005**, *50*, 2481–2486. [CrossRef]
8. Li, Z.X.; Li, X.H.; Li, W.X.; Ding, S.J. Was Cathaysia part of Proterozoic Laurentia?—New data from Hainan Island, south China. *Terra Nova* **2008**, *20*, 154–164. [CrossRef]
9. Wang, X.L.; Zhou, J.C.; Qiu, J.S.; Gao, J.F. Geochemistry of the Meso- to Neoproterozoic basic-acid rocks from Hunan Province, South China: Implications for the evolution of the western Jiangnan Orogen. *Precambrian Res.* **2004**, *135*, 79–103. [CrossRef]

10. Wang, Y.J.; Zhang, A.M.; Cawood, P.A.; Fan, W.M.; Xu, J.F.; Zhang, G.W.; Zhang, Y.Z. Geochronological, geochemical and Nd-Hf-Os isotopic fingerprinting of an early Neoproterozoic arc-back-arc system in South China and its accretionary assembly along the margin of Rodinia. *Precambrian Res.* **2013**, *231*, 343–371. [CrossRef]
11. Wang, Y.J.; Gan, C.S.; Tan, Q.L.; Zhang, Y.Z.; He, H.Y.; Qian, X.; Zhang, Y.H. Early Neoproterozoic (~840 Ma) slab window in South China: Key magmatic records in the Chencai Complex. *Precambrian Res.* **2018**, *314*, 434–451. [CrossRef]
12. Wang, W.; Zhao, J.H.; Zhou, M.F.; Pandit, M.K.; Zheng, J.P. Depositional age, provenance characteristics and tectonic setting of the Meso- and Neoproterozoic sequences in SE Yangtze Block, China: Implications on Proterozoic supercontinent reconstructions. *Precambrian Res.* **2018**, *309*, 231–247. [CrossRef]
13. Wang, W.; Zhou, M.F.; Zhao, X.F.; Chen, W.T.; Yan, D.P. Late Paleoproterozoic to Mesoproterozoic rift successions in SW China: Implication for the Yangtze Block-North Australia–Northwest Laurentia connection in the Columbia supercontinent. *Sediment. Geol.* **2014**, *309*, 33–47. [CrossRef]
14. Wang, Y.J.; Zhang, Y.Z.; Cawood, P.A.; Zhou, Y.Z.; Cui, X. Early neoproterozoic assembly and subsequent rifting in south china: Revealed from mafic and ultramafic rocks, central jiangnan orogen. *Precambrian Res.* **2019**, *331*, 105367. [CrossRef]
15. Zhou, J.C.; Wang, X.L.; Qiu, J.S.; Gao, J.F. Geochemistry of Meso- and Neoproterozoic mafic-ultramafic rocks from northern Guangxi, China: Arc or plume magmatism? *Geochem. J.* **2004**, *38*, 139–152. [CrossRef]
16. Zhou, M.F.; Ma, Y.; Yan, D.P.; Xia, X.; Zhao, J.H.; Sun, M. The Yanbian terrane (Southern Sichuan Province, SW China): A Neoproterozoic arc assemblage in the western margin of the Yangtze Block. *Precambrian Res.* **2006**, *144*, 19–38. [CrossRef]
17. Zhou, J.C.; Wang, X.L.; Qiu, J.S. Geochronology of Neoproterozoic mafic rocks and sandstones from northeastern Guizhou, South China: Coeval arc magmatism and sedimentation. *Precambrian Res.* **2009**, *170*, 27–42. [CrossRef]
18. Zhang, S.B.; Zheng, Y.F.; Wu, Y.B.; Zhao, Z.F.; Gao, S.; Wu, F.Y. Zircon U-Pb age and Hf-O isotope evidence for Paleoproterozoic metamorphic event in South China. *Precambrian Res.* **2006**, *151*, 265–288. [CrossRef]
19. Zhang, A.M.; Wang, Y.J.; Fan, W.M.; Zhang, Y.Z.; Yang, J. Earliest Neoproterozoic (ca. 1.0 Ga) arc-back-arc basin nature along the northern Yunkai Domain of the Cathaysia Block: Geochronological and geochemical evidence from the metabasite. *Precambrian Res.* **2012**, *220–221*, 217–233. [CrossRef]
20. Zheng, Y.F.; Zhang, S.B.; Zhao, Z.F.; Wu, Y.B.; Li, X.H.; Li, Z.X.; Wu, F.Y. Contrasting zircon Hf and O isotopes in the two episodes of Neoproterozoic granitoids in South China: Implications for growth and reworking of continental crust. *Lithos* **2007**, *96*, 127–150. [CrossRef]
21. Sun, M.; Chen, N.S.; Zhao, G.C.; Wilde, S.A.; Ye, K.; Guo, J.H.; Chen, Y.; Yuan, C. U-Pb Zircon and Sm-Nd isotopic study of the Huangtuling granulite, Dabie-Dulu Belt, China: Implication for the Paleoproterozoic tectonic history of the Yangtze Craton. *Am. J. Sci.* **2008**, *308*, 469–483. [CrossRef]
22. Sun, W.H.; Zhou, M.F.; Yan, D.P.; Li, J.W.; Ma, Y.X. Provenance and tectonic setting of the Neoproterozoic Yanbian Group, western Yangtze Block (SW China). *Precambrian Res.* **2008**, *167*, 213–236. [CrossRef]
23. Sun, W.H.; Zhou, M.F.; Gao, J.F.; Yang, Y.H.; Zhao, X.F.; Zhao, J.H. Detrital zircon U-Pb geochronological and Lu-Hf isotopic constraints on the Precambrian magmatic and crustal evolution of the western Yangtze Block, SW China. *Precambrian Res.* **2009**, *172*, 99–126. [CrossRef]
24. Wu, Y.B.; Zheng, Y.F.; Gao, S.; Jiao, W.F.; Liu, Y.S. Zircon U-Pb age and trace element evidence for Paleoproterozoic granulite-facies metamorphism and Archean crustal rocks in the Dabie Orogen. *Lithos* **2008**, *101*, 308–322. [CrossRef]
25. Zhao, G.C.; Cawood, P.A. Precambrian geology of China. *Precambrian Res.* **2012**, *222*, 13–54. [CrossRef]
26. Zhu, W.G.; Zhong, H.; Li, Z.X.; Bai, Z.J.; Yang, Y.J. SIMS zircon U–Pb ages, geochemistry and Nd–Hf isotopes of ca. 1.0 Ga mafic dykes and volcanic rocks in the Huili area, SW China: Origin and tectonic significance. *Precambrian Res.* **2016**, *273*, 67–89. [CrossRef]
27. Cawood, P.A.; Wang, W.; Zhao, T.Y.; Xu, Y.J.; Mulder, J.A.; Pisarevsky, S.A.; Zhang, L.M.; Gan, C.S.; He, H.Y.; Liu, H.C.; et al. Deconstructing South China and consequences for reconstructing Nuna and Rodinia. *Earth Sci. Rev.* **2020**, *204*, 103169. [CrossRef]
28. Zhao, T.Y.; Cawood, P.A.; Zi, J.W.; Wang, K.; Feng, Q.L.; Tran, D.M.; Trinh, H.D.; Dang, C.M.; Nguyen, Q.M. Positioning the Yangtze Block within Nuna: Constraints from Paleoproterozoic granitoids in North Vietnam. *Precambrian Res.* **2023**, *391*, 107059. [CrossRef]
29. Rogers, J.J.W.; Santosh, M. Configuration of Columbia, a Mesoproterozoic supercontinent. *Gondwana Res.* **2002**, *5*, 5–22. [CrossRef]
30. Torsvik, T.H. The Rodinia Jigsaw Puzzle. *Science* **2003**, *300*, 79–81. [CrossRef]
31. Cawood, P.A.; Wang, Y.J.; Xu, Y.J.; Zhao, G.C. Locating South China in Rodinia and Gondwana: A fragment of greater India lithosphere? *Geology* **2013**, *41*, 903–906. [CrossRef]
32. Li, Z.X.; Liu, Y.B.; Ernst, R. A dynamic 2000—540 Ma Earth history: From cratonic amalgamation to the age of supercontinent cycle. *Earth Sci. Rev.* **2023**, *238*, 104336. [CrossRef]
33. Cawood, P.A.; Zhao, G.C.; Yao, J.L.; Wang, W.; Xu, Y.J.; Wang, Y.J. Reconstructing South China in Phanerozoic and Precambrian supercontinents. *Earth-Sci. Rev.* **2018**, *186*, 173–194. [CrossRef]
34. Evans, D.A.D. Reconstructing pre-Pangea supercontinents. *Geol. Soc. Am. Bull.* **2013**, *125*, 1735–1751. [CrossRef]
35. Jing, X.; Evans, D.A.; Yang, Z.; Tong, Y.; Xu, Y.; Wang, H. Inverted South China: A novel configuration for Rodinia and its breakup. *Geology* **2020**, *49*, 463–467. [CrossRef]
36. Jing, X.; Yang, Z.; Evans, D.A.; Tong, Y.; Xu, Y.; Wang, H. A pan-latitudinal Rodinia in the Tonian true polar wander frame. *Earth Planet. Sci. Lett.* **2020**, *530*, 115880. [CrossRef]

37. Yao, W.H.; Li, Z.X.; Li, W.X.; Li, X.H. Proterozoic tectonics of Hainan Island in supercontinent cycles: New insights from geochronological and isotopic results. *Precambrian Res.* **2017**, *290*, 86–100. [CrossRef]
38. Zhang, L.M.; Wang, Y.J.; Qian, X.; Zhang, Y.Z.; He, H.Y.; Zhang, A.M. Petrogenesis of Mesoproterozoic mafic rocks in Hainan (South China) and its implication on the Southwest Hainan-Laurentia-Australia connection. *Precambrian Res.* **2018**, *313*, 119–133. [CrossRef]
39. Zhang, L.M.; Zhang, Y.Z.; Cui, X.; Cawood, P.A.; Wang, Y.J.; Zhang, A.M. Mesoproterozoic rift setting of SW Hainan: Evidence from the gneissic granites and metasedimentary rocks. *Precambrian Res.* **2019**, *325*, 69–87. [CrossRef]
40. Liu, H.C.; Zi, J.W.; Cawood, P.A.; Cui, X.; Zhang, L.M. Reconstructing South China in the Mesoproterozoic and its role in the Nuna and Rodinia supercontinents. *Precambrian Res.* **2020**, *337*, 72–95. [CrossRef]
41. Xu, Y.J.; Cawood, P.A.; Zhang, H.C.; Zi, J.W.; Zhou, J.B.; Li, L.X.; Du, X.S. The Mesoproterozoic Baoban Complex, South China: A missing fragment of western Laurentian lithosphere. *Geol. Soc. Am. Bull.* **2020**, *132*, 1404–1418. [CrossRef]
42. Zhou, M.F.; Yan, D.P.; Kennedy, A.; Li, Y.Q.; Ding, J. SHRIMP U–Pb zircon geochronological and geochemical evidence for Neoproterozoic arc-magmatism along the western margin of the Yangtze Block, South China. *Earth Planet. Sci. Lett.* **2002**, *196*, 51–67. [CrossRef]
43. Wang, X.L.; Shu, L.S.; Xing, G.F.; Zhou, J.C.; Tang, M.; Shu, X.J.; Qi, L.; Hu, Y.H. Post-orogenic extension in the eastern part of the Jiangnan orogen: Evidence from ca 800–760 Ma volcanic rocks. *Precambrian Res.* **2011**, *222–223*, 404–423. [CrossRef]
44. Wang, X.L.; Zhou, J.C.; Griffin, W.L.; Zhao, G.; Yu, J.H.; Qiu, J.S.; Zhang, Y.J.; Xing, G.F. Geochemical zonation across a Neoproterozoic orogenic belt: Isotopic evidence from granitoids and metasedimentary rocks of the Jiangnan orogen, China. *Precambrian Res.* **2014**, *242*, 154–171. [CrossRef]
45. Wang, Y.J.; Zhang, Y.Z.; Fan, W.M.; Geng, H.Y.; Zou, H.P.; Bi, X.W. Early Neoproterozoic accretionary assemblage in the Cathaysia Block: Geochronological, Lu-Hf isotopic and geochemical evidence from granitoid gneisses. *Precambrian Res.* **2014**, *249*, 144–161. [CrossRef]
46. Zhang, Y.Z.; Wang, Y.J. Early Neoproterozoic (~840 Ma) arc magmatism: Geochronological and geochemical constraints on the metabasites in the Central Jiangnan Orogen. *Precambrian Res.* **2016**, *275*, 1–17. [CrossRef]
47. Zhao, J.H.; Zhou, M.F.; Yan, D.P.; Zheng, J.P.; Li, J.W. Reappraisal of the ages of Neoproterozoic strata in South China: No connection with the Grenvillian orogeny. *Geology* **2011**, *39*, 299–302. [CrossRef]
48. Zhang, Y.Z.; Wang, Y.J. Early Neoproterozoic continental arc system at the central Jiangnan Orogen, South China: Geochronological and geochemical constraints on the key igneous rock-association. *Geol. Soc. Am. Bull.* **2019**, *132*, 638–654. [CrossRef]
49. Zhao, G.C.; Guo, J.H. Precambrian geology of China: Preface. *Precambrian Res.* **2012**, *222–223*, 1–12. [CrossRef]
50. Guangdong BGMR (Bureau of Geology and Mineral Resources of Guangdong). *Regional Geology of the Guangdong Province*; Geological Publication House: Beijing, China, 1988. (In Chinese with English Abstract)
51. Zhang, R.; Ma, G.; Jiang, D.; Feng, S.; Chen, M.; Xu, G.; Chen, R. *Precambrian Geology of Hainan Island, South China*; China University of Geosciences Press: Beijing, China, 1990; pp. 1–100. (In Chinese)
52. Long, W.G.; Ding, S.J.; Ma, D.Q.; Lin, Y.H.; Zhou, J.B. Formation and evolution of the precambrian basement in hainan island. *Diqiu Kexue-Zhongguo Dizhi Daxue Xuebao/Earth Sci.-J. China Univ. Geosci.* **2005**, *30*, 421–429, (In Chinese with English Abstract).
53. Xu, Y.J.; Cawood, P.A.; Du, Y.S.; Huang, H.W.; Wang, X.Y. Early Paleozoic orogenesis along Gondwana's northern margin constrained by provenance data from South China. *Tectonophysics* **2014**, *636*, 40–51. [CrossRef]
54. Yu, Z.; Shi, Y.; Yang, S. Hainan Island—A Fragment of Gondwana. In *Terrane Analysis of China and the Pacific Rim*; Wiley, T.J., Howell, D.G., Wong, F.L., Eds.; Circum-Pacific Council for Energy and Mineral Resources Earth Science Series; Circum Pacific Council Publications: Houston, TX, USA, 1990; Volume 13, pp. 283–284.
55. Yang, S.F.; Yu, Z.Y.; Guo, L.Z.; Shi, Y.S. The division and palaeomagnetism of the Hainan Island and plate tectonic significance. *J. Nanjing Univ. (Earth Sci.)* **1989**, *1*, 38–46. (In Chinese with English Abstract)
56. Metcalfe, I. Gondwanaland origin, dispersion, and accretion of East and Southeast Asian continental terranes. *J. S. Am. Earth Sci.* **1994**, *7*, 333–347. [CrossRef]
57. Metcalfe, I. Gondwanaland dispersion, Asian accretion and evolution of eastern Tethys. *Aust. J. Earth Sci.* **1996**, *43*, 605–623. [CrossRef]
58. Chen, Z.P.; Zhong, S.Z.; He, S.H.; Chen, Y.C. *Stratigraphy (Lithostratic) of Hainan Province China*; University of Geosciences Press: Wuhan, China, 1997; pp. 48–52. (In Chinese)
59. Ma, D.Q.; Huang, X.D.; Chen, Z.P.; Xiao, Z.F.; Zhang, W.C.; Zhong, S.Z. New advanced in the study of the Baoban Group in Hainan Province. *Reg. Geol. China* **1997**, *16*, 192. (In Chinese with English Abstract)
60. Wang, Z.L.; Xu, D.R.; Hu, G.C.; Yu, L.L.; Wu, C.J.; Zhang, Z.C.; Cai, J.X.; Shan, Q.; Hou, M.Z.; Chen, H.Y. Detrital zircon U-Pb ages of the Proterozoic metaclastic-sedimentary rocks in Hainan Province of South China: New constraints on the depositional time, source area, and tectonic setting of the Shilu Fe–Co–Cu ore district. *J. Asian Earth Sci.* **2015**, *113*, 1143–1161. [CrossRef]
61. Zou, S.H.; Yu, L.L.; Yu, D.S.; Xu, D.R.; Ye, T.W.; Wang, Z.L.; Cai, J.X.; Liu, M. Precambrian continental crust evolution of Hainan Island in South China: Constraints from detrital zircon Hf isotopes of metaclastic-sedimentary rocks in the Shilu Fe-Co-Cu ore district. *Precambrian Res.* **2017**, *296*, 195–207. [CrossRef]
62. Wang, X.F.; Ma, D.Q.; Jiang, D.H. *Geology of Hainan Island—Part 1: Stratigraphic Palaeontology*; Geological Publishing House: Beijing, China, 1991. (In Chinese)

63. Xia, B.D.; Ren, Z.P. Stratigraphy and sedimentary construction of Shiliu and its outlying areas on Hainan Island. *J. Nanjing Univ.* **1979**, *2*, 43–55.
64. Shan, H.Z. Study on the gold-bearing stratigraphic age in Baoban Region, Hainan province. *Acta Scifntiarum Nat. Univ. Sunyaatseni* **1990**, *29*, 71–77.
65. Ye, B.D.; Zhu, J.P. The time of the baoban group and gold ore at Erjia, Dongfang, hainan provence, china. *Contrib. Geol. Miner. Resour. Res.* **1990**, *5*, 12–17. (In Chinese with English Abstract)
66. Yu, S.J.; Xia, P.; Deng, T.Y.; Li, Q. Characteristics and U-Pb isotopic ages of zircons in the middle Proterozoic granitoids from Baoban area, Hainan province. *Geochimica* **1992**, *3*, 213–220. (In Chinese with English Abstract)
67. Hou, W.; Chen, H.F.; Liang, X.Q.; Wang, K.F. The establishment of Precambrian strata and new recognition of the geotectonic evolution in Hainan island. *J. Chang. Univ. Earth Sci.* **1992**, *22*, 143–146. (In Chinese with English Abstract)
68. Liang, X.Q. Sm-Nd ages of the Precambrian granitic-greenstone series in Hainan Island and their geological significance. *Acta Petrol. Sin.* **1995**, *11*, 71–76. (In Chinese with English Abstract)
69. Xu, D.R.; Liang, X.Q.; Cheng, G.H.; Huang, Z.L.; Hu, H.D. Research on the geochemistry and genesis of Mesoproterozoic granites on Hainan Island. *Geotecton. Metallog.* **2001**, *25*, 420–433. (In Chinese with English Abstract)
70. Xu, D.R.; Liang, X.Q.; Tang, H.F. Geochemical characteristics of metamorphic basic volcanics from the BaoBan Group, western Hainan and its tectonic implications. *Geotecton. Metallog.* **2000**, *24*, 303–313. (In Chinese with English Abstract)
71. Zhang, L.M.; Cawood, P.A.; Wang, Y.J.; Cui, X.; Zhang, Y.Z.; Qian, X.; Zhang, F.F. Provenance Record of Late Mesoproterozoic to Early Neoproterozoic Units, West Hainan, South China, and Implications for Rodinia Reconstruction. *Tectonics* **2020**, *39*, e2020TC006071. [CrossRef]
72. Hu, Z.C.; Liu, Y.S.; Gao, S.; Hu, S.H.; Dietiker, R.; Günther, D. A local aerosol extraction strategy for the determination of the aerosol composition in laser ablation inductively coupled plasma mass spectrometry. *J. Anal. At. Spectrom.* **2008**, *23*, 1192–1203. [CrossRef]
73. Liu, Y.S.; Gao, S.; Hu, Z.C.; Gao, C.G.; Zong, K.Q.; Wang, D.B. Continental and oceanic crust recycling-induced melt-peridotite interactions in the Trans-North China Orogen: U-Pb dating, Hf isotopes and trace elements in zircons of mantle xenoliths. *J. Petrol.* **2010**, *51*, 537–571. [CrossRef]
74. Ludwig, K.R. *User's Manual for Isoplot/EX Version 3.00. A Geochronological Toolkit for Microsoft Excel*; Berkeley Geochronology Center: Berkeley, CA, USA, 2003; p. 71.
75. Jackson, S.E.; Pearson, N.J.; Griffin, W.L.; Belousova, E.A. The application of laser ablation-inductively coupled plasma-mass spectrometry to in situ U-Pb zircon geochronology. *Chem. Geol.* **2004**, *211*, 47–69. [CrossRef]
76. Wiedenbeck, M.; Allé, P.; Corfu, F.; Griffin, W.L.; Meier, M.; Oberli, F.; Von Quadt, A.; Roddick, J.C.; Spiegel, W. Three natural zircon standards for U-Th-Pb, Lu-Hf, trace-element and REE analyses. *Geostand. Newsl.* **1995**, *19*, 1–23. [CrossRef]
77. Xu, D.R.; Wang, Z.L.; Chen, H.Y.; Hollings, P.; Jansen, N.H.; Zhang, Z.C. Petrography and geochemistry of the shilu Fe–Co–Cu ore district, South China: Implications for the origin of a Neoproterozoic BIF system. *Ore Geol. Rev.* **2014**, *57*, 322–350. [CrossRef]
78. Bhatia, M.R.; Crook, K.A.W. Trace element characteristics of graywackes and tectonic setting discrimination of sedimentary basin. *Contrib. Mineral. Petrol.* **1986**, *92*, 181–193. [CrossRef]
79. Bhatia, M.R. Plate tectonics and geochemical composition of sandstones. *J. Geol.* **1983**, *91*, 611–627. [CrossRef]
80. McLennan, S.M.; Taylor, S.R.; McGregor, V.R. Geochemistry of Archean metasedimentary rocks from west Greenland. *Geochim. Cosmochim. Acta* **1984**, *48*, 1–13. [CrossRef]
81. Yao, H.Z.; Sheng, X.C.; Zhang, R.J. Neoproterozoic sedimentary environment of Shilu area, Hainan Island, South China. *Gondwana Res.* **1999**, *2*, 563–566.
82. Yu, L.L.; Zou, S.H.; Cai, J.X.; Xu, D.R.; Zou, F.H.; Wang, Z.L.; Wu, C.J.; Liu, M. Geochemical and Nd isotopic constraints on provenance and depositional setting of the Shihuiding Formation in the Shilu Fe-Co-Cu ore district, Hainan Province, South China. *J. Asian Earth Sci.* **2016**, *119*, 100–117. [CrossRef]
83. Wan, Y.S.; Liu, D.Y.; Xu, M.; Zhuang, J.; Song, B.; Shi, Y.; Du, Y.L. SHRIMP U-Pb zircon geochronology and geochemistry of metavolcanic and metasedimentary rocks in Northwestern Fujian, Cathaysia Block, China: Tectonic implications and the need to redefine lithostratigraphic units. *Gondwana Res.* **2007**, *12*, 166–183. [CrossRef]
84. Shu, L.S.; Faure, M.; Yu, J.H.; Jahn, B.M. Geochronological and geochemical features of the Cathaysia block (South China): New evidence for the Neoproterozoic breakup of Rodinia. *Precambrian Res.* **2011**, *187*, 263–276. [CrossRef]
85. Zhao, G.C.; Cawood, P.A. Tectonothermal evolution of the Mayuan assemblage in the Cathaysia Block: Implications for Neoproterozoic collision-related assembly of the South China Craton. *Am. J. Sci.* **1999**, *299*, 309–339. [CrossRef]
86. Yu, J.H.; O'Reilly, S.Y.; Zhou, M.F.; Griffin, W.L.; Wang, L.J. U-Pb geochronology and Hf-Nd isotopic geochemistry of the Badu Complex, Southeastern China: Implications for the Precambrian crustal evolution and paleogeography of the Cathaysia Block. *Precambrian Res.* **2012**, *222–223*, 424–449. [CrossRef]
87. Yu, J.H.; O'Reilly, Y.S.; Wang, L.J.; Griffin, W.L.; Zhou, M.F.; Zhang, M.; Shu, L.S. Components and episodic growth of Precambrian crust in the Cathaysia Block, South China: Evidence from U–Pb ages and Hf isotopes of zircons in Neoproterozoic sediments. *Precambrian Res.* **2010**, *181*, 97–114. [CrossRef]
88. Yu, J.H.; Wang, L.J.; O'Reilly, S.Y.; Griffin, W.L.; Zhang, M.; Li, C.Z.; Shu, L.S. A Paleoproterozoic orogeny recorded in a long-lived cratonic remnant (Wuyishan terrane), eastern Cathaysia Block, China. *Precambrian Res.* **2009**, *174*, 347–363. [CrossRef]

89. Yu, J.H.; Suzanne O'Reilly, S.Y.; Wang, L.; Griffin, W.L.; Shu, L.S. Where was south china in the Rodinia supercontinent? Evidence from U-Pb geochronology and Hf isotopes of detrital zircons. *Precambrian Res.* **2008**, *164*, 1–15. [CrossRef]
90. Li, X.H.; Li, Z.X.; Li, W.X. Detrital zircon U–Pb age and Hf isotope constrains on the generation and reworking of Precambrian continental crust in the Cathaysia Block, South China: A synthesis. *Gondwana Res.* **2014**, *25*, 1202–1215. [CrossRef]
91. Li, H.K.; Zhang, C.L.; Yao, C.Y.; Xiang, Z.Q. U-Pb zircon age and Hf isotope compositions of mesoproterozoic sedimentary strata on the western margin of the Yangtze massif. *Sci. China Earth Sci.* **2013**, *56*, 628–639. [CrossRef]
92. Wang, L.J.; Yu, J.H.; Griffin, W.; O'Reilly, S. Early crustal evolution in the western Yangtze Block: Evidence from U-Pb and Lu–Hf isotopes on detrital zircons from sedimentary rocks. *Precambrian Res.* **2012**, *222–223*, 368–385. [CrossRef]
93. Cui, X.Z.; Lin, S.F.; Wang, J.; Ren, G.M.; Su, B.R.; Chen, F.L.; Deng, Q.; Pang, W.H. Latest mesoproterozoic provenance shift in the southwestern yangtze block, south china: Insights into tectonic evolution in the context of the supercontinent cycle. *Gondwana Res.* **2021**, *99*, 131–148. [CrossRef]
94. Sun, L.; Wang, W.; Pandit, M.K.; Lu, G.M.; Xue, E.K.; Huang, B.; Zhang, Y.; Wei, J.; Tian, Y. Geochemical and detrital zircon age constraints on Meso- to Neoproterozoic sedimentary basins in the southern Yangtze Block: Implications on Proterozoic geodynamics of South China and Rodinia configuration. *Precambrian Res.* **2022**, *378*, 106779. [CrossRef]
95. Sun, L.; Wang, W.; Lu, G.M.; Xue, E.K.; Huang, S.F.; Pandit, M.K.; Huang, B.; Tong, X.R.; Tian, Y.; Zhang, Y. Neoproterozoic geodynamics of south china and implications on the rodinia configuration: The Kunyang group revisited. *Precambrian Res.* **2021**, *363*, 106338. [CrossRef]
96. Fan, H.P.; Zhu, W.G.; Li, Z.X.; Zhong, H.; Bai, Z.J.; He, D.F.; Chen, C.J.; Cao, C.Y. Ca. 1.5 Ga mafic magmatism in South China during the break-up of the supercontinent Nuna/Columbia: The Zhuqing Fe-Ti-V oxide ore-bearing mafic intrusions in western Yangtze Block. *Lithos* **2013**, *168–169*, 85–98. [CrossRef]
97. Zhao, X.F.; Zhou, M.F.; Li, J.W.; Sun, M.; Gao, J.F.; Sun, W.H.; Yang, J.H. Late Paleoproterozoic to early Mesoproterozoic Dongchuan Group in Yunnan, SW China: Implications for tectonic evolution of the Yangtze Block. *Precambrian Res.* **2010**, *182*, 57–69. [CrossRef]
98. Zhou, M.F.; Zhao, X.F.; Chen, W.T.; Li, X.C.; Wang, W.; Yan, D.P.; Qiu, H.N. Proterozoic Fe-Cu metallogeny and supercontinental cycles of the southwestern Yangtze Block, southern China and northern Vietnam. *Earth Sci. Rev.* **2014**, *139*, 59–82. [CrossRef]
99. Zhao, G.C.; Cawood, P.A.; Wilde, S.A.; Sun, M. Review of global 2.1–1.8 Ga orogens: Implications for a pre-Rodinia supercontinent. *Earth Sci. Rev.* **2002**, *59*, 125–162. [CrossRef]
100. Zhao, G.C.; Sun, M.; Wilde, S.A.; Li, S.Z. A Paleo-Mesoproterozoic supercontinent: Assembly, growth and breakup. *Earth Sci. Rev.* **2004**, *67*, 91–123. [CrossRef]
101. Evans, D.A.D.; Mitchell, R.N. Assembly and breakup of the core of Paleoproterozoic-Mesoproterozoic supercontinent Nuna. *Geology* **2011**, *39*, 443–446. [CrossRef]
102. Ross, G.M.; Parrish, R.R.; Winston, D. Provenance and U-Pb geochronology of the Mesoproterozoic Belt Supergroup (northwestern United States): Implications for age of deposition and pre-Panthalassa plate reconstructions. *Earth Planet. Sci. Lett.* **1992**, *113*, 57–76. [CrossRef]
103. Evans, K.; Aleinikoff, J.N.; Obradovich, J.D.; Fanning, C.M. SHRIMP U-Pb geochronology of volcanic rocks, Belt Supergroup, western Montana: Evidence for rapid deposition of sedimentary strata. *Can. J. Earth Sci.* **2000**, *37*, 1287–1300. [CrossRef]
104. Ross, G.M.; Villeneuve, M. Provenance of the Mesoproterozoic (1.45 Ga) Belt basin (western North America): Another piece in the pre-Rodinia paleogeographic puzzle. *Geol. Soc. Am. Bull.* **2003**, *115*, 1191–1217. [CrossRef]
105. Stewart, E.D.; Link, P.K.; Fanning, C.M.; Frost, C.D.; McCurry, M. Paleogeographic implications of non-North American sediment in the Mesoproterozoic upper Belt Supergroup and Lemhi Group, Idaho and Montana, USA. *Geology* **2010**, *38*, 927–930. [CrossRef]
106. Doe, M.F.; Jones, J.V.; Karlstrom, K.E.; Dixon, B.; Gehrels, G.; Pecha, M. Using detrital zircon ages and Hf isotopes to identify 1.48–1.45 Ga sedimentary basins and fingerprint sources of exotic 1.6–1.5 Ga grains in southwestern Laurentia. *Precambrian Res.* **2013**, *231*, 409–421. [CrossRef]
107. Doe, M.F.; Jones, J.V.; Karlstrom, K.E.; Thrane, K.; Frei, D.; Gehrels, G.; Pecha, M. Basin formation near the end of the 1.60–1.45 Ga tectonic gap in southern Laurentia: Mesoproterozoic Hess Canyon Group of Arizona and implications for ca. 1.5 Ga supercontinent configurations. *Lithosphere* **2012**, *4*, 77–88. [CrossRef]
108. Rämö, O.T.; McLemore, T.; Hamilton, M.A.; Kosunen, P.J.; Heizler, M.; Haapala, I. Intermittent 1630–1220 Ma magmatism in central Mazatzal province: New geochronologic piercing points and some tectonic implications. *Geology* **2003**, *31*, 335–338. [CrossRef]
109. Medig, K.P.R.; Thorkelson, D.J.; Davis, W.J.; Rainbird, R.H.; Gibson, H.D.; Turner, E.C.; Marshall, D.D. Pinning northeastern Australia to northwestern Laurentia in the Mesoproterozoic. *Precambrian Res.* **2014**, *249*, 88–99. [CrossRef]
110. Link, P.K.; Fanning, C.M.; Lund, K.I.; Aleinikoff, J.N. Detrital zircons, correlation and provenance of Mesoproterozoic Belt Supergroup and correlative strata of eastcentral Idaho and southwest Montana. *Proterozoic Geol. West. N. Am. Sib. Spec. Publ.* **2007**, *86*, 101–128.
111. Fanning, C.M.; Reid, A.; Teale, G.S. A geochronological framework for the Gawler Craton, South Australia. *S. Aust. Geol. Surv. Bull.* **2007**, *55*, 258.
112. Hand, M.; Reid, A.; Jagodzinski, E. Tectonic framework and evolution of the Gawler Craton, southern Australia. *Econ. Geol.* **2007**, *102*, 1377–1395. [CrossRef]

113. Reid, A.; Hand, M.; Jagodzinski, E.; Kelsey, D.; Pearson, N. Paleoproterozoic orogenesis in the southeastern Gawler Craton, South Australia. *J. Geol. Soc. Aust.* **2008**, *55*, 449–471. [CrossRef]
114. Belousova, E.A.; Reid, A.J.; Griffin, W.L.; O'Reilly, S.Y. Rejuvenation vs. recycling of Archean crust in the Gawler Craton, South Australia: Evidence from U-Pb and Hf isotopes in detrital zircon. *Lithos* **2009**, *113*, 570–582. [CrossRef]
115. Howard, K.E.; Hand, M.; Barovich, K.M.; Belousova, E. Provenance of late Paleoproterozoic cover sequences in the central Gawler Craton: Exploring stratigraphic correlations in eastern Proterozoic Australia using detrital zircon ages, Hf and Nd isotopic data. *J. Geol. Soc. Aust.* **2011**, *58*, 475–500. [CrossRef]
116. Reid, A.J.; Payne, J.L. Magmatic zircon Lu-Hf isotopic record of juvenile addition and crustal reworking in the Gawler Craton, Australia. *Lithos* **2017**, *292–293*, 294–306. [CrossRef]
117. Peucat, J.J.; Capdevila, R.; Fanning, C.M.; MéNot, R.P.; PéCora, L.; Testut, L. 1.60 Ga felsic volcanic blocks in themoraines of the Terre Adélie Craton, Antarctica: Comparisons with the Gawler range volcanics, South Australia. *J. Geol. Soc. Aust.* **2002**, *49*, 831–845.
118. Goodge, J.W.; Fanning, C.M.; Brecke, D.M.; Licht, K.J.; Palmer, E.F. Continuation of the Laurentian Grenville province in western East Antarctica. *J. Geol.* **2010**, *118*, 601–619. [CrossRef]
119. Goodge, J.W.; Fanning, C.M.; Fisher, C.M.; Vervoort, J.D. Proterozoic crustal evolution of central East Antarctica: Age and isotopic evidence from glacial igneous clasts, and links with Australia and Laurentia. *Precambrian Res.* **2017**, *299*, 151–176. [CrossRef]
120. Liu, X.C.; Zhao, Y.; Chen, H.; Song, B. New zircon U–Pb and Hf–Nd isotopic constraints on the timing of magmatism, sedimentation and metamorphism in the northern Prince Charles Mountains, East Antarctica. *Precambrian Res.* **2017**, *299*, 15–33. [CrossRef]
121. Liu, X.C.; Wang, W.; Zhao, Y.; Liu, J.; Chen, H.; Cui, Y.C.; Song, B. Early Mesoproterozoic arc magmatism followed by early Neoproterozoic granulite facies metamorphism with a near-isobaric cooling path at Mount Brown, Princess Elizabeth Land, East Antarctica. *Precambrian Res.* **2016**, *284*, 30–48. [CrossRef]
122. Paulsen, T.; Deering, C.; Sliwinski, J.; Bachmann, O.; Guillong, M. New detrital zircon age and trace element evidence for 1450 Ma igneous zircon sources in East Antarctica. *Precambrian Res.* **2017**, *300*, 53–58. [CrossRef]
123. Anderson, H.E.; Davis, D.W. U-Pb geochronology of the Moyie sills, Purcell Supergroup, southeastern British Columbia: Implications for the Mesoproterozoic geological history of the Purcell (Belt) basin. *Can. J. Earth Sci.* **1995**, *32*, 1180–1193. [CrossRef]
124. Frost, C.D.; Frost, B.R. Reduced rapakivi-type granites: The tholeiite connection. *Geology* **1997**, *25*, 647–650. [CrossRef]
125. Frost, C.D.; Frost, B.R.; Bell, J.M.; Chamberlain, K.R. The relationship between A-type granites and residual magmas from Anorthosite: Evidence from the northern Sherman batholith, Laramie mountains, Wyoming, USA. *Precambrian Res.* **2002**, *119*, 45–71. [CrossRef]
126. Goodge, J.W.; Vervoort, J.D. Origin of Mesoproterozoic A-type granites in Laurentia: Hf isotope evidence. *Earth Planet. Sci. Lett.* **2006**, *243*, 711–731. [CrossRef]
127. Link, P.K.; Stewart, E.D.; Steel, T.; Sherwin, J.-A.; Hess, L.T.; McDonald, C. Detrital zircons in the Mesoproterozoic upper Belt Supergroup in the Pioneer, Beaverhead and Lemhi Ranges, Montana and Idaho: The Big White arc. *Geol. Soc. Am. Spec. Pap.* **2016**, *522*, 163–183.
128. Mulder, J.A.; Karlstrom, K.E.; Fletcher, K.; Heizler, M.T.; Timmons, J.M.; Crossey, L.J.; Gehrels, G.E.; Pecha, M. The syn-orogenic sedimentary record of the Grenville Orogeny in southwest Laurentia. *Precambrian Res.* **2017**, *294*, 33–52. [CrossRef]
129. Malone, D.H.; Craddock, J.P.; Link, P.K.; Foreman, B.Z.; Scroggins, M.A.; Rappe, J. Detrital zircon geochronology of quartzite clasts, northwest Wyoming: Implications for Cordilleran Neoproterozoic stratigraphy and depositional patterns. *Precambrian Res.* **2017**, *289*, 116–128. [CrossRef]
130. Wang, W.; Cawood, P.A.; Pandit, M.K.; Xia, X.P.; Zhao, J.H. Coupled precambrian crustal evolution and supercontinent cycles: Insights from in-situ U-Pb, O- and Hf-isotopes in detrital zircon, NW India. *Am. J. Sci.* **2018**, *318*, 989–1017. [CrossRef]
131. McKenzie, N.R.; Hughes, N.C.; Myrow, P.M.; Xiao, S.; Sharma, M. Correlation of Precambrian–Cambrian sedimentary successions across northern India and the utility of isotopic signatures of Himalayan lithotectonic zones. *Earth Planet. Sci. Lett.* **2011**, *312*, 471–483. [CrossRef]
132. McKenzie, N.R.; Hughes, N.C.; Myrow, P.M.; Banerjee, D.M.; Deb, M.; Planavsky, N.J. New age constraints for the Proterozoic Aravalli-Delhi successions of India and their implications. *Precambrian Res.* **2013**, *238*, 120–128. [CrossRef]
133. Malone, S.J.; Meert, J.G.; Banerjee, D.M.; Pandit, M.K.; Tamrat, E.; Kamenov, G.D.; Pradhan, V.R.; Sohl, L.E. Paleomagnetism and detrital zircon geochronology of the upper Vindhyan sequence, Son Valley and Rajasthan, India: A ca 1000 Ma closure age for the Purana basins? *Precambrian Res.* **2008**, *164*, 137–159. [CrossRef]
134. Turner, C.C.; Meert, J.G.; Pandit, M.K.; Kamenov, G.D. A detrital zircon U–Pb and Hf isotopic transect across the son valley sector of the vindhyan basin, india: Implications for basin evolution and paleogeography. *Gondwana Res.* **2014**, *26*, 348–364. [CrossRef]
135. Ahäll, K.I.; Connelly, J. Intermittent 1.53–1.13 Ga magmatism in western Baltica; age constraints and correlations within a postulated supercontinent. *Precambrian Res.* **1998**, *92*, 1–20. [CrossRef]
136. Condie, K.C.; Belousova, E.; Griffin, W.; Sircombe, K.N. Granitoid events in space and time: Constraints from igneous and detrital zircon age spectra. *Gondwana Res.* **2009**, *15*, 228–242. [CrossRef]
137. Condie, K.C.; O'Neill, C.; Aster, R.C. Evidence and implications for a widespread magmatic shutdown for 250 My on Earth. *Earth Planet. Sci. Lett.* **2009**, *282*, 294–298. [CrossRef]

138. Zhang, S.H.; Zhao, Y.; Liu, X.C.; Liu, Y.S.; Hou, K.J.; Li, C.F.; Ye, H. U–Pb geochronology and geochemistry of the bedrocks and moraine sediments from the Windmill Islands: Implications for Proterozoic evolution of East Antarctica. *Precambrian Res.* **2012**, *206–207*, 52–71. [CrossRef]
139. Stark, J.C.; Wang, X.C.; Li, Z.X.; Rasmussen, B.; Sheppard, S.; Zi, J.W.; Clark, C.; Hand, M.; Li, W.X. In situ U-Pb geochronology and geochemistry of a 1.13 Ga mafic dyke suite at Bunger Hills, East Antarctica: The end of the Albany-Fraser Orogeny. *Precambrian Res.* **2018**, *310*, 76–92. [CrossRef]
140. Gaál, G.; Gorbatschev, R. An outline of the Precambrian Evolution of the Baltic Shield. *Precambrian Res.* **1987**, *35*, 15–52. [CrossRef]
141. Bogdanova, S.; Gorbatschev, R.; Skridlaite, G.; Soesoo, A.; Taran, L.; Kurlovich, D. Trans-Baltic Palaeoproterozoic correlations towards the reconstruction of supercontinent Columbia/Nuna. *Precambrian Res.* **2015**, *259*, 5–33. [CrossRef]
142. Morrissey, L.J.; Payne, J.L.; Hand, M.; Clark, C.; Taylor, R.; Kirkland, C.L.; Kylander-Clark, A. Linking the windmill islands, East Antarctica and the Albany–Fraser Orogen: Insights from U–Pb zircon geochronology and Hf isotopes. *Precambrian Res.* **2017**, *293*, 131–149. [CrossRef]

Disclaimer/Publisher's Note: The statements, opinions and data contained in all publications are solely those of the individual author(s) and contributor(s) and not of MDPI and/or the editor(s). MDPI and/or the editor(s) disclaim responsibility for any injury to people or property resulting from any ideas, methods, instructions or products referred to in the content.